3'

AURORAL ZONE ELECTRIC FIELDS FROM DE-1 AND -2 AT MAGNETIC CONJUNCTIONS

by

Daniel Ray Weimer

A thesis submitted in partial fulfillment
of the requirements for the Doctor of
Philosophy degree in Physics
in the Graduate College of
The University of Iowa

December 1984

Thesis supervisor: Professor Donald A. Gurnett

Graduate College
The University of Iowa
Iowa City, Iowa

CERTIFICATE OF APPROVAL

PH.D. THESIS

This is to certify that the Ph.D. thesis of

Daniel Ray Weimer

has been approved by the Examining Committee for the thesis requirement for the Doctor of Philosophy degree in Physics at the December 1984 graduation.

Thesis committee: Daniel A. Hewett
Thesis supervisor

N R Malik
Member

Christopher K. Ross
Member

J.A. Van Allen
Member

W D'Angelo
Member

ACKNOWLEDGEMENTS

I thank my thesis supervisor, Dr. Gurnett, for his guidance during the past year. I also thank Dr. Goertz for the valuable discussions on the theories related to this work, and Dr. Shawhan for giving me the opportunity to work as a part of the Dynamics Explorer Science Team.

I thank the Science Team investigators who have sent me essential data from the other instruments on DE-1 and DE-2, particularly Drs. Nelson Maynard, Masahisa Sugiura, Jim Burch, Doug Menietti, Bill Peterson, and Ed Shelley. Credit is also due to Dr. Bob Hoffman for his management of the DE Project.

I thank: Rich Huff, for getting the Plasma Wave Instrument electric field data transferred to Iowa City. Terry Averkamp, for programming assistance, especially with the routines needed to read the DE-2 electric field data. Kathy Kurth, for the excellent typing of the thesis. Joyce Chrisinger and John Birkbeck, for their artwork, without which there would be no figures in this thesis. Mark Brown, for his prompt and dependable processing of the microfilm plots.

I should mention Dr. J. D. Goddard, whom it was my pleasure to have as a teacher while I was an undergraduate at the University of Michigan (he is now at UCLA). Without his encouragement (and letter

of recommendation) it is unlikely that I would have chosen to go to graduate school, so this thesis would never have been written.

Special credit is also due to the Transplant Staff at the University of Iowa Hospitals and Clinics. Without their efforts, and the kidney from an unknown donor, it would not have been possible for me to attend graduate school.

I thank Masahisa Sugiura at the Goddard Space Flight Center for providing the measurements from the magnetometer on DE-1. The research at the University of Iowa was supported by NASA through grant NAG5-310 from Goddard Space Flight Center, grants NGL-16-001-043 and NGL-16-001-002 from NASA Headquarters, and grant N00014-76-C-0016 from the Office of Naval Research.

ABSTRACT

Nearly simultaneous measurements of auroral zone electric fields are obtained by the Dynamics Explorer spacecraft at altitudes below 900 km and above 4,500 km during magnetic conjunctions. The measured electric fields are approximately perpendicular to the magnetic field lines. The north-south meridional electric fields are "projected" to a common altitude by a mapping function. When plotted as a function of invariant latitude, graphs of the projected electric fields measured by DE-1 and DE-2 show that the large-scale electric field is the same at both altitudes. However, superimposed on the large-scale fields are small-scale features with wavelengths less than 100 km which are larger in magnitude at the higher altitude. Fourier transforms of the electric fields show that the magnitudes depend on wavelength. Outside of the auroral zone the electric field spectrums are nearly identical. But within the auroral zone the spectrums of the high and low altitude electric fields have a ratio which increases with the reciprocal of the wavelength. The small-scale electric field variations are associated with field-aligned currents. These currents are measured with both a plasma instrument and magnetometer on DE-1. The spectrum of the east-west magnetic field component measured on the high altitude satellite is found to be nearly identical to the spectrum of the north-south electric

field measured on the low altitude satellite, with a ratio that is independent of wavelength. This ratio is proportional to the ionospheric conductivity.

The experimental measurements are found to agree with a steady-state theory which postulates that there are parallel potential drops associated with the variations in the perpendicular electric fields. It is assumed that there is a linear relationship between the field-aligned current and the total parallel potential drop, and that the field-aligned currents close through Pedersen currents in the ionosphere. The theory predicts that the ratio between the low and high altitude electric fields varies with the wavelength. Due to the excellent agreement between the theory and observations, it is concluded that the linear relationship between the current density and potential drop is a good approximation.

TABLE OF CONTENTS

LIST OF PLATES

LIST OF FIGURES

I. INTRODUCTION

Electric fields in the auroral zone have been the subject of numerous theoretical and experimental investigations for more than two decades. From a phenomenological point of view, the objective of this work has been to reach an understanding of what causes the aurora. On the physical level, this reduces to determining the electrodynamical processes associated with field-aligned currents and particle precipitation.

The two Dynamics Explorer (DE) spacecraft were launched in August of 1981 for the purpose of investigating the auroral phenomena and other processes in the earth's magnetosphere and ionosphere. DE-1 makes measurements primarily in the magnetosphere; the orbit is highly elliptical, with perigee at 675 km altitude (1.106 R_e) and apogee at 23,250 km (4.65 R_e). DE-2 orbits in the upper ionosphere at altitudes of 305 to 1000 km. The spacecraft are in coplanar polar orbits, so at times of magnetic conjunctions between the two spacecraft it is possible to obtain simultaneous measurements of fields and particles at different altitudes on a magnetic field line.

The purpose of this paper is to present the results of a study of quasi-static electric fields in the auroral zone. Data from both DE spacecraft are used, from orbits in which there was a magnetic conjunction between 50° and 80° Invariant Latitude.

II. PREVIOUS RESULTS

There have been high expectations that the Dynamics Explorer program would help to answer many of the questions about auroral processes which have yet to be resolved. The primary problem is the relationship between field-aligned currents and electric fields, both parallel and perpendicular to the magnetic field lines. In a space plasma the magnetic field lines are generally considered to be perfect conductors, and thus have the same electric potential at all points along their length. There should be no potential drops parallel to the field lines, and electric fields perpendicular to the field lines should vary inversely with the distance separating neighboring magnetic field lines. On the basis of rocket and satellite measurements of charged particles which had been accelerated along the field lines, it has long been assumed that parallel electric fields must somehow exist in the auroral zone [Stern, 1983]. Without these electric fields auroral arcs could not be produced.

Theoretical models of auroral zone electric fields and electric potentials have been discussed in numerous papers. Among the more recent papers are those by Lyons [1980, 1981], Chiu and Cornwall [1980], Chiu et al. [1981]. The main emphasis of these papers is the relationship between field-aligned currents and parallel potential

drops. The field-aligned current is due to an enlargement of the "loss cone" due to a parallel potential drop in a region above the point where the particles normally are reflected by the "mirror force." From an equation given by Knight [1973], Lyons [1980] shows that, with some restrictions, there is an approximately linear relationship between the current and the parallel potential difference. The field line conductance is shown to depend on the electron density and the thermal energy. An isotropic Maxwellian electron distribution is assumed, although Chiu et al. [1981] show that the "kinetic Ohm's law" holds for an arbitrary electron distribution function. In these papers by Lyons and Chiu et al., it is shown that the regions with a parallel potential drop should have a natural perpendicular scale length of about 100 km. The value of this scale length is determined by the conductances of both the ionosphere and the magnetic field lines.

Parallel electric fields distributed along a field line for thousands of kilometers cannot be measured directly by one satellite, although they have been inferred from a statistical study. Mozer and Tobert [1980] used the electric fields measured by one satellite at different altitudes over a long period of time to show that the average electric field is larger at higher altitudes.

The large-scale perpendicular electric fields measured on low-altitude satellites are found to correlate well with orthogonal magnetic field measurements [Smiddy et al., 1980; Burke et al., 1982; Sugiura et al., 1982; Sugiura, 1984]. This correlation requires a

steady-state situation in which there are no field-aligned potential drops and that field-aligned currents close in the ionosphere by Pedersen currents rather than Hall currents. The ratio between E and B is then determined by the height-integrated Pedersen conductivity.

On a much smaller spatial scale (a few tens of kilometers), very large electric fields with amplitudes up to 1 V/m have been measured with the S3-3 satellite [Mozer et al., 1977]. These large fields often have the structure of oppositely directed perpendicular fields. Parallel electric fields are reported to be found within these structures, which are interpreted as being due to stationary double layers or "electrostatic shocks." Numerous subsequent reports of the S3-3 electric field data and its interpretation are summarized by Mozer et al. [1980].

Additional reviews of the nature of the large electric fields in the auroral zone are presented by Stern [1981, 1983] and Shawhan et al. [1978]. Candidate mechanisms for the generation of parallel electric fields include anomalous resistivity, thermoelectric effect, magnetic mirror effect, and double layers (shocks). A comparison of magnetic field (current) data and electric field data may be important in deciding which theory or combination of theories are correct. The S3-3 satellite lacked the capability to determine the magnetic field or current structure on the same size scale as the "electrostatic shocks" which were detected, so a comparison between E and B was not possible.

Time-dependent models of auroral field lines are discussed in papers by Hasegawa [1976], Mallinckrodt and Carlson [1978], Goertz and Boswell [1979], Lysak and Hudson [1979], Lysak and Carlson [1981], and Lysak and Dum [1983]. The common feature of these theories is the coupling of the magnetosphere and ionosphere with Alfven waves propagating along auroral field lines.

In the latter three papers the effects of "microscopic turbulence" on the wave propagation are discussed. The introduction of turbulence causes a static parallel electric field to be generated. This would explain the time evolution of the stationary model proposed by Mozer et al. Possible detections of Alfven waves are presented by Aggson et al. [1983], Gelpi and Bering [1984], Dubinin et al. [1984], and Gurnett et al. [1984]. These investigations were in frequency ranges of .1 Hz, .5 Hz, 1 Hz, and 2-100 Hz, respectively. It is also interesting that Arnoldy et al. [1983] report evidence for Alfven waves on the basis of ground observations of optical auroral and magnetic fields at magnetically conjugate locations.

III. INSTRUMENTATION AND DATA ANALYSIS

The objective of the Dynamics Explorer mission is to investigate the processes which couple the earth's magnetosphere and ionosphere and the effects of the solar wind on the space plasma around the earth. Two satellites are used in order to obtain simultaneous measurements far away from the earth in the magnetosphere and just above the ionosphere. Specific details about the program, spacecraft configuration, etc., are provided by Hoffman et al. [1981a,b].

The major emphasis of this paper is the quasi-static electric fields measured by the Plasma Wave Instrument (PWI) on DE-1 and the Vector Electric Field Instrument (VEFI) on DE-2.

A double floating probe technique is used to determine the electric field by measuring the difference of the floating potentials of identical probes located in symmetric positions relative to the body of the spacecraft. Details about this technique can be found in the papers by Fahleson [1967] and by Cauffman and Gurnett [1972]. Electric fields are measured in the spin-orbit plane of DE-1 with a 200 m tip-to-tip long wire antenna. (DE-1 spins at a rate of one revolution in six seconds around an axis which is perpendicular to the orbit plane.) The electric field is sampled at a rate of 16 samples per second. Due to the rotation of the spacecraft, a static

electric field will appear in the "raw' data as a sine wave with a six-second period. The magnitude and direction of the electric field component in the spin-orbit plane are determined with a least-squares fit of the data to a sine wave. Segments of data spanning six seconds of time are used for each measurement of the electric field. The segments which are used for adjacent measurements are overlapped in time by two seconds. This results in a measurement of the electric field at four-second intervals. Complete details of the Plasma Wave Instrument design are provided by Shawhan et al. [1981]. The techniques used to analyze the quasi-static electric field data are documented by Weimer [1983].

Electric fields are measured on the DE-2 spacecraft by two orthogonal double probes in the orbit plane (a third probe in the direction of the orbit normal failed to deploy properly after launch). The antennas are of a self-supporting tubular type measuring 22.4 m tip-to-tip. DE-2 rotates only once per orbit, resulting in a constant orientation of the antennas with respect to the direction of motion. The data rate is 16 samples per second; all VEFI data shown in this paper are averages of 8 samples at 1/2-second intervals. Further information about the VEFI can be found in the paper by Maynard et al. [1981]. With both the DE-1 and DE-2 data, there is an electric field due to $\underline{V}_{sc} \times \underline{B}$, where $\underline{V}_{sc}$ is the spacecraft velocity relative to corotation and $\underline{B}$ is the magnetic field of the earth. The $\underline{V}_{sc} \times \underline{B}$ electric fields are subtracted from the data to obtain the ambient electric field in a reference frame corotating with the earth.

In this paper data are used from additional instruments, which are vital to the understanding of the role of electric fields in the auroral processes. Magnetic field data are obtained from a triaxial fluxgate magnetometer (MAGA) described in detail by Farthing et al. [1981]. The sampling rate is 16 vector samples per second. From the derivative of the magnetic field it is possible to compute the field aligned current density.

The velocity-space distribution of electrons and positive ions over the energy range of 5 eV to 32 keV are obtained from the High Altitude Plasma Instrument (HAPI). This instrument consists of five electrostatic analyzers which have different viewing angles relative to the spacecraft spin axis. The detailed description of this instrument is found in the paper by Burch et al. [1981]. Of particular significance to the present study are the measured values of current and energy flux carried by particles moving up and down the magnetic field lines.

Measurements of ion composition and energy pitch-angle distributions are obtained from the Energetic Ion Composition Spectrometer (EICS). Refer to the paper by Shelly et al. [1981] for the instrument description. The data from the instrument can show the pitch-angle distributions of ions flowing up the field lines. Ions with a high field-aligned velocity are indicative of a parallel potential below the DE-1 spacecraft.

IV. OBSERVATIONS

A. General Characteristics

The electric field measurements from DE-1 and DE-2 indicate that the auroral zone is characterized by intense, variable electric fields. Large magnitude variations are sometimes seen in regions only 10 to 50 kilometers wide, in agreement with the observations published before the launch of the Dynamics Explorers.

A description of these fields as measured near the ionosphere with the VEFI on DE-2 has previously been published by Maynard et al. [1982b]. It was concluded that the field variability previously observed at higher altitudes sometimes penetrates down into the ionosphere more than previously suspected. Although the field magnitudes measured on DE-2 occasionally exceed 100 mV/m, the variability is less than would be produced if the high altitude structures [Gurnett and Frank, 1977; Mozer et al., 1977; Maynard et al., 1982a] were projected to DE-2 altitudes, assuming the magnetic field lines are equipotentials.

The Plasma Wave Instrument on the DE-1 spacecraft measures the electric fields at a wide range of altitudes, due to the highly elliptical orbit. An example of how the measured fields vary at different parts of the DE-1 orbit is shown in Figure 1. This is an 80-minute plot of the peak electric fields measured with the 200 m

long wire antenna which rotates within the orbit plane. The maximum and minimum values measured during each spin period are plotted on the graph, thereby showing the envelope of the sine wave impressed on the data by the antenna's rotation in the quasi-static electric fields. The pass through the auroral zone in the northern hemisphere is distinctly visible between 3:40 and 3:55 UT. There is a pronounced enhancement in the magnitude and variability of the fields during this time period. Most of the variations are of a moderate magnitude (10-50 mV/m) and have a spatial extent of over 100 kilometers. However, in this example there is one very prominent "spike" with a magnitude over 150 mV/m which did not persist for much longer than one spin period. Intense (over 100 mV/m), narrow (less than 12 seconds or 60 km wide) spikes of this nature are found in approximately 10% of the passes through the auroral zone at distances between 1.7 and 4 R_e. High resolution graphs which show every data point (16 samples per second) reveal that the electric fields at the large spikes usually reverse directions. This reversal is characteristic of the "shocks" reported by Mozer et al. [1977].

When DE-1 passes through the auroral zone at low altitudes the large electric field variations are very rarely observed. In the example in Figure 1 the spacecraft reaches perigee in the southern hemisphere at 4:30 UT. Most of the field which is measured is due to the $\underline{V}_{sc} \times \underline{B}$ electric field. The calculated value of the spin plane component of $\underline{V}_{sc} \times \underline{B}$ is shown as the smooth curve superimposed on the peak field plot; $\underline{B}$ is derived from the Magsat model [Langel et al.,

1980]. In the two auroral zone crossings going to and from the pole near perigee there are very few variations superimposed on the field due to $\underline{V}_{sc} \times \underline{B}$. The stair-step appearance in the peak field plot is due to the fact that the electric field data are obtained from two separate differential amplifiers. Relatively small electric fields are digitized at high-resolution (0.14 mV/m) with a high-gain amplifier. Fields above 58 mV/m saturate this amplifier, so data are obtained from a low-gain amplifier at a more coarse digital resolution (14 mV/m). However, for the least squares fit analysis the high resolution data are used during the majority of the spin period when the antenna is not aligned with the electric field.

B. Comparative Studies

In principle, two spacecraft at different altitudes on the same magnetic field line should measure the same perpendicular electric field if there are no parallel electric fields between the spacecraft. In order to compare to DE-1 and DE-2 electric field measurements, the data can be plotted as a function of invariant latitude (the latitude, in magnetic coordinates, at which the field line the spacecraft is on intersects the surface of the earth). For such a comparison it is also necessary to account for the fact that the field line separation changes with altitude. This is accomplished with a mapping function which "projects" the measured electric fields to a common altitude.

An example of perpendicular electric fields measured in the orbit plane by both DE spacecraft near a conjunction is shown in Figure 2. The solid curve is the field measured by the PWI on DE-1. The data points are spaced apart in time by four seconds. The dashed line is the electric field measured by the VEFI on DE-2. These data points are obtained at half-second intervals from an average of eight digital samples. The data are projected to a common radial distance of 1 R_e and plotted as a function of invariant latitude. The projection or mapping formula assumes that the magnetic field lines are equipotentials, i.e., there are no electric fields parallel to the magnetic field. Therefore, the mapping function for electric fields perpendicular to the magnetic field is determined by the dipole field line geometry. For electric fields in the meridional plane the relationship between the measured field and the projected field is:

$$E_p = E_m L \sqrt{4L - 3} \frac{\cos^3\lambda_m}{(\cos^2\lambda_m + 4\sin^2\lambda_m)^{1/2}} \tag{1}$$

where λ_m is the magnetic latitude at the measurement point, L is the McIlwain parameter equal to $1/\cos^2\lambda_o$, and λ_o is the invariant latitude. Figure 2 shows that the two spacecraft measure nearly identical electric fields at the same invariant latitudes. Note that there is a three- to four-minute time difference between the two spacecraft. The primary purpose of showing this figure is to demonstrate

that the electric field comparison can be accomplished. In order to succeed, the measurement techniques, the subtraction of $\underline{V} \times \underline{B}$, the projection formula, and the orbit data must be correct. The electric fields seen in this example are mainly due to the double-cell plasma convection pattern which is often seen over the polar cap [Cauffman and Gurnett, 1972]. On this day the convection velocity was unusually large. A convection reversal occurs at 69° Inv. Field-aligned currents are presumed to exist on the equatorward side of the reversal where the fields measured by DE-1 and DE-2 deviate from each other. In this example, DE-1 was near perigee; the most useful comparisons are found when DE-1 is at higher altitudes, in which case the number of data points per degree of invariant latitude may match or exceed the resolution of DE-2. The drawback is that there will be greater time differences, since DE-1 may move through a 15° span of invariant latitude in 40 minutes while DE-2 will take just five minutes.

A comparison of the projected electric fields with DE-1 at an altitude of 8,000 to 10,000 km is shown in Figure 3. The DE-1 data are from part of the same orbit which was shown in Figure 1. Although there are differences in the magnetic local time ranging from 0.4 to 0.6 hours and a 12- to 22-minute time difference between the passage of the spacecraft through this region, there are similar features in both curves. However, it is evident that most of the variations with a small spatial length have a much larger magnitude at the higher altitude spacecraft. As a general trend observed on

many similar graphs of projected electric fields, the small-scale variations are superimposed upon a large-scale electric field pattern which is very much alike at the two different spacecraft altitudes.

In order to compare the magnitude of the electric fields measured at high and low altitudes as a function of spatial wavelength, the data are processed with a discrete Fourier transform (a Cooley-Tukey FFT algorithm is employed). The data are transformed for a common span of invariant latitude. As the electric field data are sampled at discrete time intervals, the FFT yields a power spectrum which is sampled at discrete frequencies. As the time interval required for the spacecraft to transverse the specified range of invariant latitude is known, the frequencies can be converted to wavelengths. In comparing the electric field spectrums at different altitudes it is convenient to use the reciprocal of the wavelength projected to the base of the field line at 1 R_e.

Figure 4 is the result of Fourier transforming the data shown in Figure 3 for the section of invariant latitude ranging from 62° to 67°, where most of the high-altitude electric field variations are found. (Note that the spectrums show electric field magnitudes rather than the more conventional spectral densities). Using the same convention as in the projected field plot, the solid line represents the DE-1 spectrum and the dashed line shows the DE-2 spectrum. The Fourier transform was performed on the mapped values of the electric field. At the lowest wavenumbers (very large wavelengths) the electric field magnitudes agree very well. But at wavelengths less

than 150 km the electric fields are larger at the higher altitude (solid line) than at the lower altitude (dashed line). Therefore, the smaller-scale structures do not "map" along the field lines. This is a feature common to many of the electric field spectrums in the auroral zone.

The differences between the high and low altitude electric field spectrums are most pronounced when there is a large flux of electron energy into the ionosphere, so that the height-integrated Pedersen ionospheric conductivity is high. For this particular case, the electron data from the High Altitude Plasma Instrument (HAPI) are shown in Figure 5. An enhanced energy flux is evident from 3:42 to 3:52 UT. At the top of the graph are the ionospheric conductivities which are estimated on the basis of the flux of the electrons going down to the ionosphere. Rapid variations in the parallel velocity and current density are also indicated.

More accurate measurements of the field-aligned current density are obtained from measurements of the magnetic field; Figure 6 shows the east-west component (ΔB_ϕ) measured with the magnetometer on DE-1. The background field due to the earth's dipole has been subtracted from the measured magnetic field. The resulting field variations are believed to be caused by motion of the spacecraft through field-aligned currents. The current density, calculated from the rate of change of the magnetic field and the spacecraft velocity, is also shown in Figure 6. As these graphs are a function of time rather than invariant latitude, for purposes of comparison the DE-1 electric field data (without mapping) are included in Figure 6.

At altitudes just above the ionosphere the north-south electric field and east-west magnetic field are related by the ionospheric conductivity [Smiddy et al., 1980]:

$$\frac{\Delta B_y}{E_x} = 1.256\ \Sigma_p \quad . \tag{2}$$

ΔB_y is the difference between the measured magnetic field and the dipole field in units of nano-Tesla, E_x is the electric field in millivolts/meter, and Σ_p is the height-integrated Pedersen conductivity in units of mhos. A constant ratio between ΔB_y and E_x is also expected at higher altitudes due to the mapping of both E and B (the scaling of B is governed by conservation of current in a magnetic flux tube). The E and B in Figure 6 do not appear to be related at all. However, in Fourier analyzing the magnetic field for the very same time period as the DE-1 electric field, the results shown in Figure 7 are obtained. The magnetic field spectrum measured on DE-1 is shown superimposed on the electric field spectrum measured on DE-2. The figure shows that the ratio between the two spectrums is nearly constant, with a value of 9 nT/mVm^{-1}. This ratio can be used to compute the ionospheric conductivity. The magnetic field used to compute the spectrum in Figure 7 had been multiplied by the very same mapping factor as the DE-1 electric field in order to keep constant the ratio of E to B measured at the DE-1 satellite. To obtain the actual mapped value of B it should be multiplied by an additional

factor in order to account for the convergence of the field lines in the longitudinal direction. The projected east-west magnetic field is obtained from the measured value by:

$$B_p = B_m L^{3/2} \cos^3 \lambda_m \tag{3}$$

$$B_p = B_m \frac{E_p}{E_m} \left(\frac{1 + 3\sin^3\lambda_m}{1 + 3\sin^2\lambda_o}\right)^{1/2} \quad . \tag{4}$$

For the case at hand the additional correction factor is 0.88. The Pedersen conductivity calculated from the DE-1 magnetometer spectrum and the DE-2 electric field spectrum is 6 mhos. This is a reasonable value, but less than that predicted by HAPI data in Figure 5.

Another case for study is introduced in Figure 8 (day 303, 1981). The range of invariant latitude for which the data are shown is much wider than in the previous example. As before, there are similarities in the underlying features, but the DE-1 data show many large-amplitude variations of narrow width. The spectrum for 65° to 70° invariant latitude is shown in Figure 9. Again, there is good correlation at large wavelengths and a dramatic divergence in the magnitudes as the wavelength decreases.

Simultaneous data from the HAPI and magnetometer for day 303, 1981 are shown in Figures 10 and 11. The spectrum of the magnetic

field for 65° to 70° Inv. is in Figure 12. The results are nearly the same as in the previous case. In the region where the most variations are found in the high altitude electric field, there is an enhanced electron energy flux. The current density is variable, though predominately upward. The spectrum of the east-west magnetic field at the high altitude is nearly identical to (by a constant factor) the spectrum of the electric field at the low altitude. With an adjustment factor of 0.87 (from Equation (4)), the Pedersen conductivity calculated from the ratio of B to E is 11 mhos. This agrees well with the HAPI data in Figure 10.

A pitch-angle spectrogram from the Energetic Ion Spectrometer (EICS) in Plate 1 indicates that during this pass through the auroral zone there were ion beams coming up the field line from the ionosphere, some with energies over 1 keV. This implies a parallel electric field between the ionosphere and DE-1. The ion beams are seen between 13:23 and 13:37 UT at the 90° pitch angle. During the time at which these data were obtained, the time resolution of the EICS is 96 seconds, so it is difficult to correlate any particular feature in the electric field data with any peaks in the ion beams.

In Figure 8 it is seen that the two DE spacecraft measure nearly identical electric fields after leaving the auroral zone. The spectrograms in Figure 13 show that the electric field spectral density has a power law behavior, with $E^2 \sim k^{-1.8}$. Nearly the same power law was measured outside of the auroral zone by Kintner [1976] for plasma turbulence occurring in the frequency range of 1 to 100 Hz; Kintner

must have been measuring the continuation of the spectrum in Figure 13 at the high frequency range. The power law measured here is in close agreement with a theory credited to Kolmogorov [Batchelor, 1970]. In a three-dimensional "fluid" being stirred at wave number k_o, energy flows toward larger wave numbers with the spectrum $E^2(k) \sim k^{-5/3}$. In Figure 13 the electric field at the largest wavelength (smallest wavenumber) is due to the polar cap convection driven by the solar wind. This is the source of the turbulence which propagates toward the large wavenumbers.

A summary of average electric fields measured by both DE-1 and DE-2 is presented in Figure 14. The data are from 18 different crossings through the range of 50° to 80° invariant latitude, chosen for the occurrence of a conjunction within this range. The spacecraft are determined to be at a conjunction according to computations based on the Magsat model of the earth's magnetic field [Langel et al., 1980]. Using this model and the spacecraft coordinates, the field lines on which the spacecraft are located are traced down to their intersection with the earth's surface. A conjunction is defined to occur whenever the difference between the bases of the field lines is less than 3° latitude and 6° longitude.

For the 18 cases used in Figure 14, DE-1 was at radial distances above 1.7 R_e, at an average altitude of 12,400 km. The average altitude of DE-2 was 800 km. The data had been Fourier analyzed, then divided into 4 different wavelength ranges before averaging. It is

evident that at the largest wavelengths the data from DE-1 and DE-2 agree very well, but at the smallest wavelengths the electric fields measured by DE-1 in the auroral zone are larger than those measured by DE-2.

In Figure 15 the data from 65° to 70° are used in a graph of the average electric field as a function of $1/\lambda$. In this case the data had been divided into 8 different frequency "bins" before averaging. The ratio of the electric fields measured by DE-2 and DE-1 is shown in addition to the magnitudes. This graph shows the same general trends in the electric field spectrums as was evident in the individual cases shown earlier.

V. INTERPRETATION

The observations reported here indicate that electric field variations found in the auroral zone have a "mapping" function that depends on the wavelength of the variations. The large-scale electric fields, in general due to the polar cap plasma convection pattern, have the same magnitude at high and low altitudes. In contrast, the small-scale variations associated with the aurora have a larger magnitude at high altitudes. This indicates that there must be a magnetic field aligned (parallel) potential drop associated with the smaller features. This is consistent with the discrete nature of auroral arcs.

In a previously published study by Mozer and Torbert [1980] it was concluded that there exists a large-scale parallel potential, about three degrees wide, centered around 69° or 70° invariant latitude. This conclusion was based on the average electric field measured by the S3-3 satellite at different altitudes.

By inclusion of the large magnitude "spikes" in the averaging process, the high altitude data naturally had a higher average magnitude. In contrast, by using a Fourier transform to determine the electric field magnitudes as a function of wavelength, the summary of the Dynamics Explorer data in Figure 14 shows that there is not a wide scale parallel potential drop. Instead, an average of the

electric field measurements between 65° and 70° (Figure 15) indicates that the ratio of electric fields at low and high altitudes has a wavelength dependence.

In the individual cases examined here, where it is known that significant field-aligned currents were present, there is seen to be a much more distinct wavelength dependence in the ratio between the low and high altitude electric fields. There is a sharp break in the ratio, occurring at wavelengths of 90-200 km. This agrees with the "scale lengths" of discrete auroral arcs. Mathematical models of auroral field lines, developed by Lyons [1980, 1981] and Chiu et al. [1981] have predicted such scale lengths. The key point in these papers is the use of a linear "Ohms law" relationship between the field-aligned current density and the total parallel potential drop which occurs on the field lines. Before the launch of the Dynamics Explorer satellites it was not possible to experimentally verify the theories in a relatively direct manner.

It can be shown that the DE electric field data which has been presented here does support the theory. The crucial steps in this investigation are the Fourier transform of electric field measurements which have been projected to a common altitude, and the conversion of the Fourier transform from a frequency domain to a wavenumber domain, where the wavelengths have also been projected to a common altitude. In effect, this maps the fields from a "dipole" coordinate system to a cartesian coordinate system, illustrated in Figure 16. The z axis is in the direction of the magnetic field; z increases

with altitude. $z = i$ is taken to be the top of the ionosphere. The x axis is in the north-south direction. It is assumed that there is little variation in the east-west direction, so that the problem is two-dimensional. As auroral arcs are generally very long in the east-west direction, this is usually a valid assumption. The parallel potential drop from the DE-1 spacecraft at $z = h$ to the DE-2 spacecraft at $z = i$ is $V_{\parallel}$.

The following mathematical derivation was developed by Goertz [personal communication, 1984], following the same techniques used by Lyons, with the addition of a Fourier transform. From the steady state current continuity equation

$$\nabla \cdot \overline{j} = 0 \tag{5}$$

and Ohms law

$$\overline{j} = \overline{\sigma} \cdot \overline{E} \tag{6}$$

the current in the ionosphere, $j_{\parallel}(z)$, is related to the electric field by

$$\frac{\partial}{\partial z} j_{\parallel}(z) = - \frac{\partial}{\partial x} \sigma_x E_x(z) \quad . \tag{7}$$

Integrating in the z direction from the bottom of the conducting ionosphere to z = i yields

$$j_{\parallel}^{i} = -\Sigma_{p} \frac{\partial E_{x}^{i}}{\partial x} \tag{8}$$

$$\frac{j_{\parallel}^{i}}{\Sigma_{p}} = -\frac{\partial E_{x}^{i}}{\partial x} \tag{9}$$

where Σ_p is the height-integrated Pedersen ionospheric conductivity.

Above the ionosphere, no current can be conducted perpendicular to the field lines (the x direction). In the direction of the field lines, the presence of a parallel potential drop implies that there is an "anomalous resistivity," or non-infinite conductance. Calling this conductance "a", the Ohms law relationship between $j_{\parallel}$ and $V_{\parallel}$ is [Lyons, 1980; Chiu et al., 1981]:

$$J_{\parallel} = -aV_{\parallel} \quad . \tag{10}$$

The sign convention is such that $j_{\parallel}$ is positive (away from the ionosphere) when the electric potential at z = i is greater than the potential at z = h.

Equations (9) and (10) can be combined to give

$$\frac{aV_{\parallel}}{\Sigma_p} = \frac{\partial E_x^i}{\partial x} \quad . \tag{11}$$

From Maxwell's equation:

$$\overline{\nabla} \times \overline{E} = 0 \tag{12}$$

$$\frac{\partial E_x}{\partial z} = \frac{\partial E_z}{\partial x} \tag{13}$$

$$\int_i^h \frac{\partial E_x}{\partial z} dz = \frac{\partial}{\partial x} \int_i^h E_z dz \tag{14}$$

$$E_x^h - E_x^i = - \frac{\partial}{\partial x} V_{\parallel} \tag{15}$$

$$E_x^i = E_x^h + \frac{\partial}{\partial x} V_{\parallel} \tag{16}$$

Substituting this expression for E_x^i into Equation (11) results in

$$\frac{aV_{\parallel}}{\Sigma_p} = \frac{\partial^2 V_{\parallel}}{\partial x^2} + \frac{\partial E_x^h}{\partial x} \quad . \tag{17}$$

With the definition of a constant factor,

$$\frac{a}{\Sigma_p} \equiv k_o^2 \tag{18}$$

and the fact that E_x can be defined as the negative derivative of a potential, Equation (17) becomes

$$\frac{\partial^2 V_\parallel}{\partial x^2} - k_o^2 V_\parallel = \frac{\partial^2 \phi_x^h}{\partial x^2} \quad . \tag{19}$$

The potential function ϕ_x can be expanded in a Fourier series:

$$\phi_x^h \equiv \sum_k \phi_k^h \, e^{ikx} \tag{20}$$

$$E_x^h \equiv \sum_k \left(- ik\phi_k^h \, e^{ikx}\right) \quad . \tag{21}$$

The solution to the differential Equation (19) is:

$$V_\parallel = [Ae^{k_o x} + Be^{-k_o x}] + \sum_k \left(\frac{k^2}{k^2 + k_o^2} \phi_k^h e^{ikx}\right) \quad . \tag{22}$$

Substituting this solution for $V_\parallel$ back into Equation (16) while using the relation (21), the ionospheric electric field is:

$$E_x^i = E_x^h - \frac{k^2 E_x^h}{k^2 + k_o^2} + k_o[Ae^{+k_o x} + Be^{-k_o x}] \quad . \tag{23}$$

For E_x^i to remain finite at all values of x requires that A = B = 0. The resulting relationship between the ionospheric and high-altitude electric field, for each Fourier component with wavenumber k, is

$$E_x^i = \frac{k_o^2}{k^2 + k_o^2} E_x^h \quad . \tag{24}$$

The relationship between the electric field and magnetic field is derived from:

$$\overline{\nabla} \times \overline{B} = \mu_o \overline{j} \tag{25}$$

$$\frac{\partial B_y}{\partial x} = \mu_o j_{\parallel} \quad . \tag{26}$$

From Equations (10) and (22):

$$\frac{1}{\mu_o} \frac{\partial B_y}{\partial x} = -a \sum_k \left(\frac{k^2}{k^2 + k_o^2} \phi_k^h e^{ikx}\right) \tag{27}$$

$$B_y = \frac{a\mu_o}{k^2 + k_o^2} E_x^h = \frac{k_o^2}{k^2 + k_o^2} \mu_o \Sigma_p E_x^h = \mu_o \Sigma_p E_x^i \quad . \tag{28}$$

Thus we recover the same constant relationship between B_y and E_x^i which was previously given in Equation (2). Similarly, it can be shown that there is a relationship between the current density and the high-altitude electric field:

$$j_\parallel = + i \frac{k\, k_o^2}{k^2 + k_o^2} \Sigma_p E_x^h \tag{29}$$

$$j_\parallel = \frac{+k_o^2}{k^2 + k_o^2} \Sigma_p \frac{\partial E_x^h}{\partial x} \tag{30}$$

The equation which we are most interested in is (24), which indicates that an electric field with an infinite wavelength ($k = 0$) has the same magnitude at high and low altitudes. As the wavelength decreases (k increases) the ratio of the ionospheric electric field to the high altitude field decreases. At values of k above k_o the ratio falls off as $1/k^2$. This prediction can be tested with the experimental data. One difficulty arises due to the fact that the discrete spectrums computed with the FFT appear to "zig-zag" around

the actual values, which should (more or less) follow a smooth curve. A sliding average can be used to smooth the spectrums.

Figures 17 and 18 show the ratio of the electric fields measured by DE-2 and DE-1 for the two different cases which have been discussed previously. The spectrums had been smoothed with a four-point sliding average before computing the ratios. The dashed lines show the ratio of the electric fields computed with Equation (25), in which k_o has been chosen to give the best visual fit to the data. The agreement between the data and the theory is quite good. It must be remembered that the results are based on the Fourier transform of several minutes worth of data, during which time all of the parameters may not be constant. For example, the Pedersen conductivity shown in Figures 5 and 10 shows some variability. This variability could account for the scatter in the data about the theoretical values. At the wavenumbers higher than those for which data values are shown in Figures 17 and 18, the trend does not fit the theory.

Another test of the agreement between the data and the theory follows from Equation (29). In Figures 19 and 20 are shown the ratio between $j_\parallel$ and E_x^h as a function of wavelength. Since the current density is obtained from the derivative of the magnetic field, the Fourier transform of the current is equal to the Fourier transform of the magnetic field multiplied by the wavenumber. The dots show the ratio $j_\parallel/E_x^h$ obtained from the smoothed magnetic field and electric field spectrums. All data are from DE-1. The dashed lines show the theoretical curves from Equation (20). The values of k_o were taken

from Figures 17 and 18 and the values of Σ_p were obtained from Figures 7 and 12. The result is a fairly good match with the experimental data.

From the values of k_o determined by the best fit, the field line conductance can be computed from Equation (18), using the previously determined values of Σ_p. In the case on day 296, 1981, the value of "a" is $3.2 \cdot 10^{-8}$ mho/m^2. For day 303, 1981, the conductance is computed to be $1.6 \cdot 10^{-8}$ mho/m^2. Lyons [1981] shows the the conductance should be related to the electron density and thermal energy according to

$$a = 2.7 \cdot 10^{-8} \frac{n}{k_{th}^{1/2}} \frac{\text{mho}}{\text{m}^2} \tag{31}$$

where n has units of cm^{-3} and k_{th} has units of eV. For a "typical" density of 1 cm^{-3} and a thermal energy of 250 eV, the expected value of the conductance is $1.7 \cdot 10^{-9}$ mho/m^2. For the cases discussed here these parameters in principle can be measured by the HAPI electron detector. However, photoelectrons from the surface of the spacecraft interfere with the counting of the lowest energy electrons. In both of these cases, if electrons with energies less than 23 eV are included in the calculations, the conductances are estimated to be 10^{-7} mho/m^2. If the low energy electrons are excluded from the calculations, the conductances are 10^{-9} mho/m^2. Therefore, the conductances inferred from the electric and magnetic field

measurements, which lie between these two extreme values, appear to be very reasonable.

The total potential drop can be computed from:

$$V_{\parallel} = - \frac{i\,k}{k^2 + k_o^2} E_x^h \quad . \tag{32}$$

The potential drop $V_{\parallel}$ has a maximum value (with respect to k) of $E_x^h/2k_o$. In the case from Day 296, 1981, k_o corresponds to a "wave" which spans 0.75° of invariant latitude. In Figure 3 there is a feature in the DE-1 electric field plot (at 65.5°) which has this wavelength and a magnitude of ~ 100 mV/m. This "wave" would have an associated potential drop of 660 volts. In the case from Day 303, 1981, where k_o appears to be smaller, an electric field with a magnitude of 100 mV/m and a wavelength of k_o would have an associated potential drop of 1,300 volts. Thus, the ion beams with energies over 1 keV which were detected by the EICS (Plate 1) can be accounted for. It is interesting that the electric field spikes with the largest magnitudes occur where $k > k_o$ and therefore are associated with voltage drops of a lower magnitude. For instance, in Figure 8 it is evident that the high altitude electric field has several spikes with projected magnitudes over 200 mV/m at wavenumbers on the order of $2 \cdot 10^{-4}$ m^{-1}. As k_o has a value of $3.8 \cdot 10^{-5}$ m^{-1}, these spikes would be associated with potential drops of 900 volts.

The agreement between the electric field data and Equation (24) indicates that the Ohms law approximation is valid. One assumption

upon which Equation (10) is based is that $V_{\parallel}$ must be the total potential drop along the magnetic field line from the ionosphere to the magnetic equator. In order for the observations to match the theory DE-1 must be above the region where the total potential drop is located; i.e., potential drops above the high altitude satellite must be small.

In both the specific cases and the averages of multiple passes through the auroral zone (Figure 15), the ratio of E_2/E_1 does not fit the general trend (nor the theory) at the largest wavenumbers. There are two possible explanations. It is likely due to the fact that the least-square-fit analysis of the high-altitude electric field data tends to reduce in magnitude the variations which have very small wavelengths. The second explanation is that there may be second-order effects which appear at high wavenumbers. The Pedersen conductivity may have a wavelength dependence, Equation (10) may have a small nonlinear term, or plasma waves may have an effect.

The equations shown here are an expression of the electrodynamic processes which occur on auroral field lines at the macroscopic level. At the microscopic level, a mechanism is required to produce the field-aligned electric fields which are implied to exist. As discussed by both Stern [1983] and Shawhan et al. [1978], there are a number of theories: anomalous resistivity, magnetic mirror effect, double layers, and wave-particle interactions. The results presented in this paper are consistent with the magnetic mirror effect, although it is possible that a combination of mechanisms are involved.

VI. CONCLUSION

Electric field measurements have been presented from both Dynamics Explorer satellites near magnetic conjunctions. In order to remove the variations caused by the dipole magnetic field line geometry, the electric fields which are measured at different altitudes are projected to a common altitude. Graphs of projected electric fields plotted as a function of invariant latitude show that the large scale features are the same at high and low altitudes. This is especially true outside of the auroral zone, where the electric fields measured by DE-1 and DE-2 are nearly identical. The auroral zone, in contrast, is marked by small-scale variations which appear to have a much larger magnitude at higher altitudes. The difference in the magnitude implies that there are parallel, field-aligned potential drops associated wtih the smaller structures.

In order to quantify the differences in the electric fields, the data are Fourier analyzed. This analysis shows how the electric field magnitudes depend on wavelength.

Outside of the auroral zone the high and low altitude electric fields show nearly identical power laws. The spectral index is found to be nearly the same as had been measured by Kintner [1976] at much higher frequencies. The power law is presumed to be due to plasma turbulence, with energy cascading from small to large wavenumbers.

The source of the energy at the smallest wavenumber is believed to be the polar-cap plasma convection which is driven by the solar wind.

Within the auroral zone the Fourier analysis indicates that the ratio of the electric fields measured at low and high altitudes has a wavelength dependence. The difference between the electric field spectrums is most pronounced in cases where there is a large flux of electrons moving down the field lines and the ionospheric conductivity is high.

Previous reports in the literature had indicated that at low altitudes there is a correlation between the north-south electric field and the east-west magnetic field. The east-west magnetic field measured on the high altitude DE-1 satellite is found to be correlated with the electric field measured at the low-altitude DE-2 satellite. The ratio between E_x and B_y is a measurement of the height-integrated Pedersen ionospheric conductivity. The magnetic field measured on DE-1 appears to have little correlation with the electric field measured on DE-1. Instead, large current densities, indicated by dB_y/dx, occur in the regions where dE_x/dx is also large.

The observational data are found to be in good agreement with a mathematical model of the auroral zone electric fields. The starting point for the theory is an assumed linear relationship between the current density and field-aligned total potential drop. It had been shown by Lyons and Chiu et al. that this should be a valid approximation. With the use of the steady-state form of Maxwell's equations and a Fourier expansion of the electric fields, it is shown here

that the ratio of low altitude/high altitude electric fields does have a wavelength dependence. A "critical" wavenumber, k_o, is found that depends on the ratio of the parallel field-line conductivity and the ionospheric Pedersen conductivity. Electric field variations which have this wavenumber are associated with the largest potential drops. Electric field amplitudes with wave numbers larger than k_o are not effectively transferred from high to low altitudes.

To summarize, there are several key assumptions which have been made in this analysis. They are: 1. The two spacecraft are measuring fields on the same magnetic field lines. 2. The fields are stationary. 3. The ionospheric conductivity is constant in the north-south (x) direction. 4. The fields do not vary significantly in the east-west (y) direction. 5. There is a linear relationship between the magnetic field-aligned current density and the total field-aligned voltage drop. It is useful to briefly discuss the validity of these assumptions.

The definition of a "magnetic conjunction" has been applied rather loosely in this work. The two spacecraft, which are moving at different velocities, can be at a true conjunction only for a brief instant in time. However, for this study the most important requirement is that the two spacecraft fly through the same part of the aurora while conditions are similar, which helps to eliminate major temporal effects.

A steady-state situation has been assumed in both the data analysis and theoretical models. It is also well known that

individual "auroral arcs" do move back-and-forth in the north-south direction. This movement makes it difficult to compare electric/magnetic fields measured at different altitudes on a point for point basis, but the movement should not affect the ratios of the fields determined by the spectral analysis. The movement is considered to be slow enough that the use of the time-independent Maxwell's equations in the theory is justified. If the time-variations were an important factor, then the ratio of B_y to E_x measured on DE-1 should be governed by the Alfven speed. If this were the case, then the electric field (mV/m) variations would be approximately 10 to 30 times larger than the corresponding magnetic field (nT) variations. Instead, the electric field is about 10 times smaller than the magnetic field.

A constant ionospheric conductivity is assumed, although the conductivities calculated from the electron flux are variable. There are distinct regions where the electron flux and conductivity are greater than the adjacent regions. By doing the data analysis (Fourier transform) for a time period in which the general character of the electron flux is the same, the influence of the variable conductivity is hopefully reduced. The smaller variations within this region may be responsible for the "scatter" of the measured quantities around the theoretical curves.

With the assumption that there are little variations in the east-west direction, the analysis is reduced to two dimensions. This implies that the field-aligned currents are in the form of infinite

sheets. Ground observations of auroral arcs and spacecraft measurements of magnetic fields indicate that this is usually a good approximation. Also, there would not be a good correlation between the north-south electric field and east-west magnetic field if this were not the case. The lack of variability in the east-west direction may be explained by conservation of the second adiabatic invariant. The plasma in the earth's magnetic field is inhibited in moving across "shells" of constant invariant latitude but may drift freely (and equalize parameters) in the east-west direction.

The linear relationship between the current and potential is the most important assumption in the comparison between theory and experiment. In considering that in this type of experimental work all parameters cannot be carefully controlled, the results show an excellent agreement between the measurements and the theory. It can be concluded that the Ohms law approximation is valid.

Plate 1 Ion flux vs. 'spin phase angle' and time, from the Energetic Ion Composition Spectrometer on DE-1, Day 303, 1981. The flux has been integrated from 1 keV/e to 17 keV/e. The m/q values of 1, 16, and 4 correspond to H^+, O^+, and He^+, respectively. Zero degrees pitch angle corresponds to the "ram" direction, and ~ 90° to ions flowing up field lines from below. The classic loss cones for the high energy ions are clearly visible after ~ 13:38 UT. Note the presence of ion "beams" coming up the field line between ~ 13:23 and 13:37 UT. The flux units color coded by the bar on the right are $(cm^2\text{-sec-sr})^{-1}$.

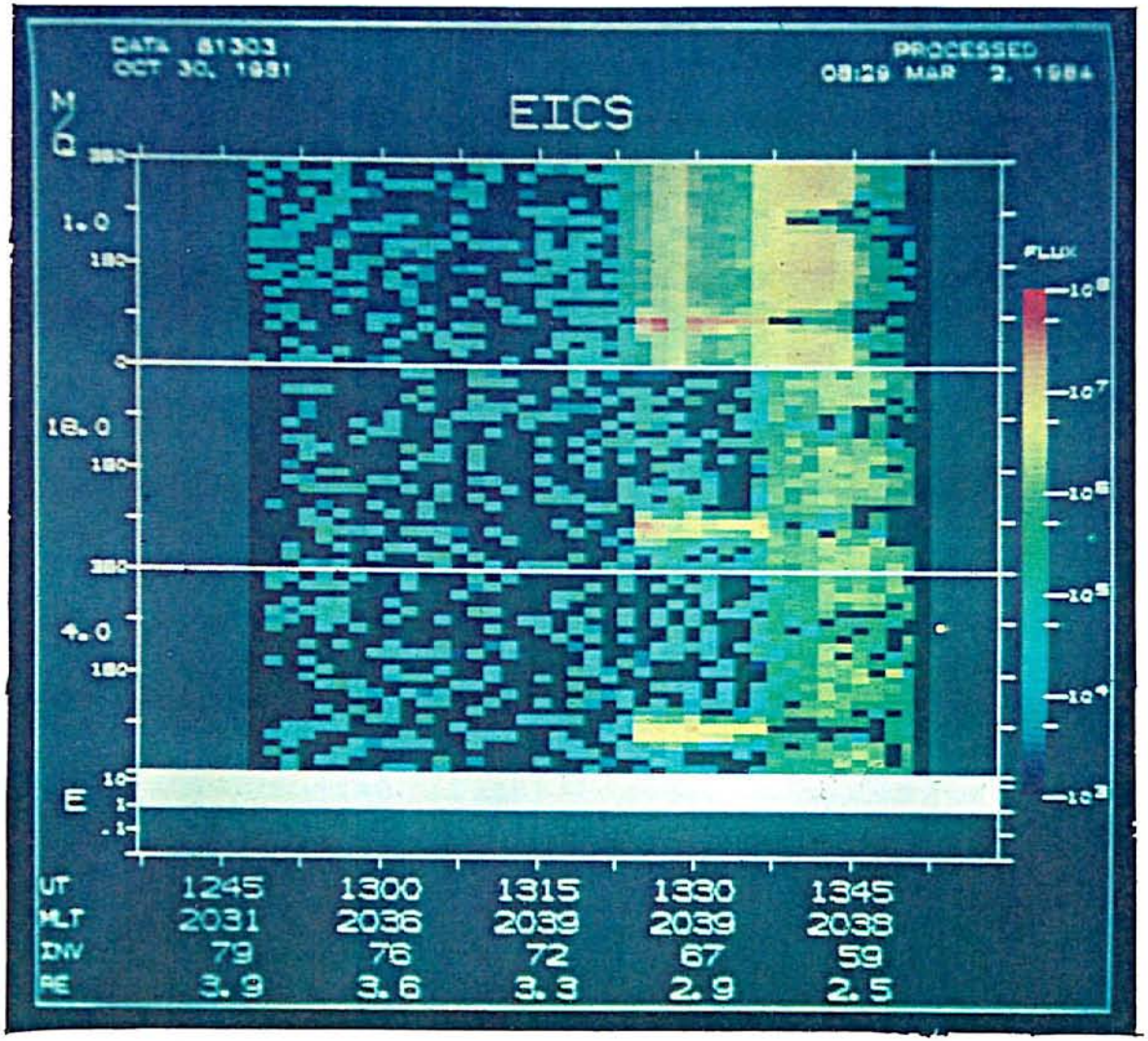
DATA 81303
OCT 30, 1981
PROCESSED
08:29 MAR 2, 1984
EICS
M/Q
1.0
18.0
4.0
E
FLUX
UT 1245 1300 1315 1330 1345
MLT 2031 2036 2039 2039 2038
INV 79 76 72 67 59
RE 3.9 3.6 3.3 2.9 2.5

Plate 1

Figure 1 Graph of peak electric fields measured by the DE-1 Plasma Wave Instrument on October 23, 1981. The passage of the spacecraft through the "auroral zone in the northern hemisphere is indicated by the variations in the electric field between 3:40 UT and 3:55 UT. In contrast, the auroral zone crossings in the southern hemisphere near perigee (680 km altitude) do not show such large variations. Most of the electric field measured at the low altitude is due to the movement through the earth's magnetic field. The stair-step appearance at large magnitudes is due to the digitization of the data.

A-G84-842

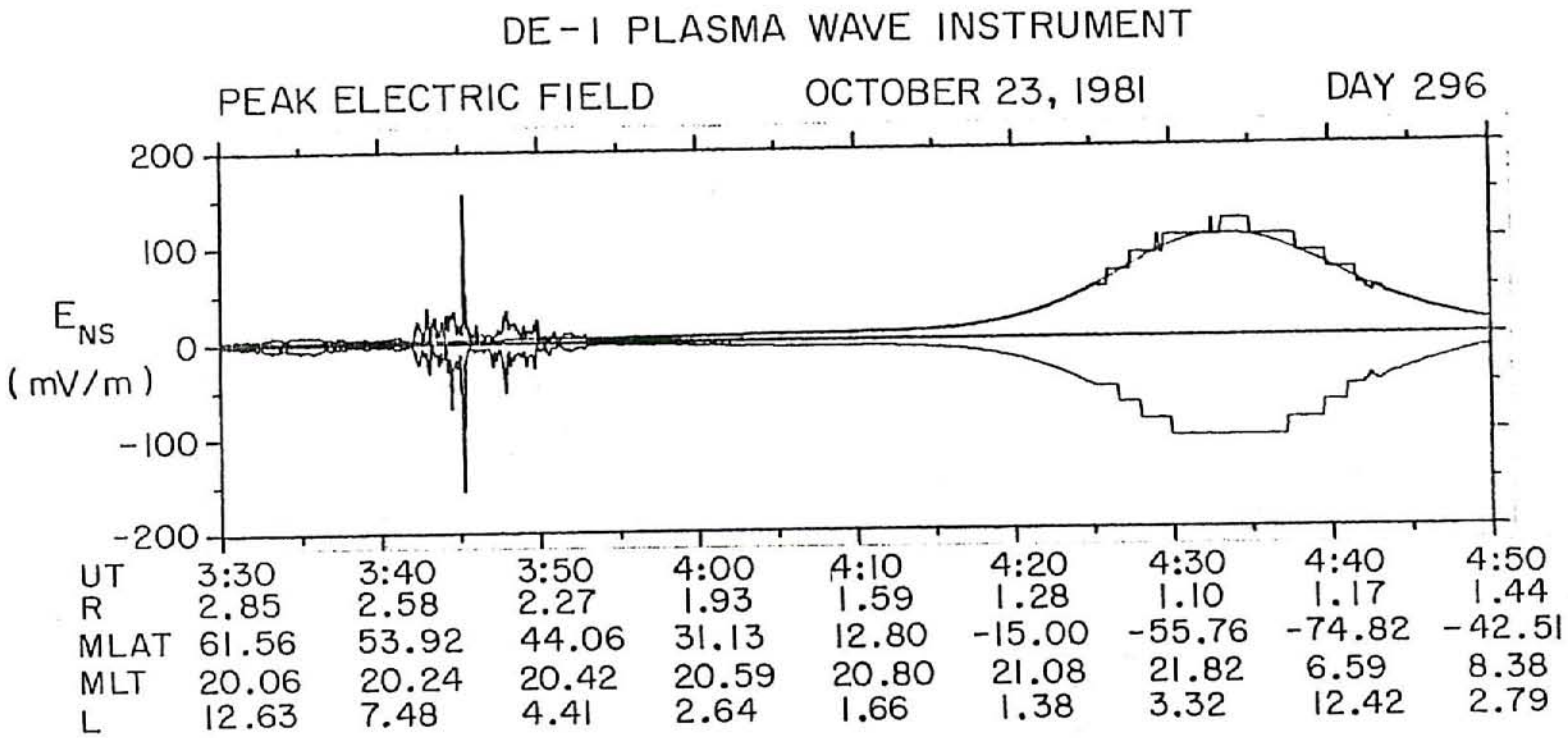

Figure 1

Figure 2 Projected electric fields measured by DE-1 and DE-2 on day 364 (December 30), 1981. The solid line shows the electric field measured by DE-1; the dashed line shows the values measured by DE-2. The measured electric fields are projected to a common radial distance of 1 R_e and plotted as a function of invariant latitude. Positive values are in the direction of motion, which is from south to north in this case. The times are rounded to the nearest minute.

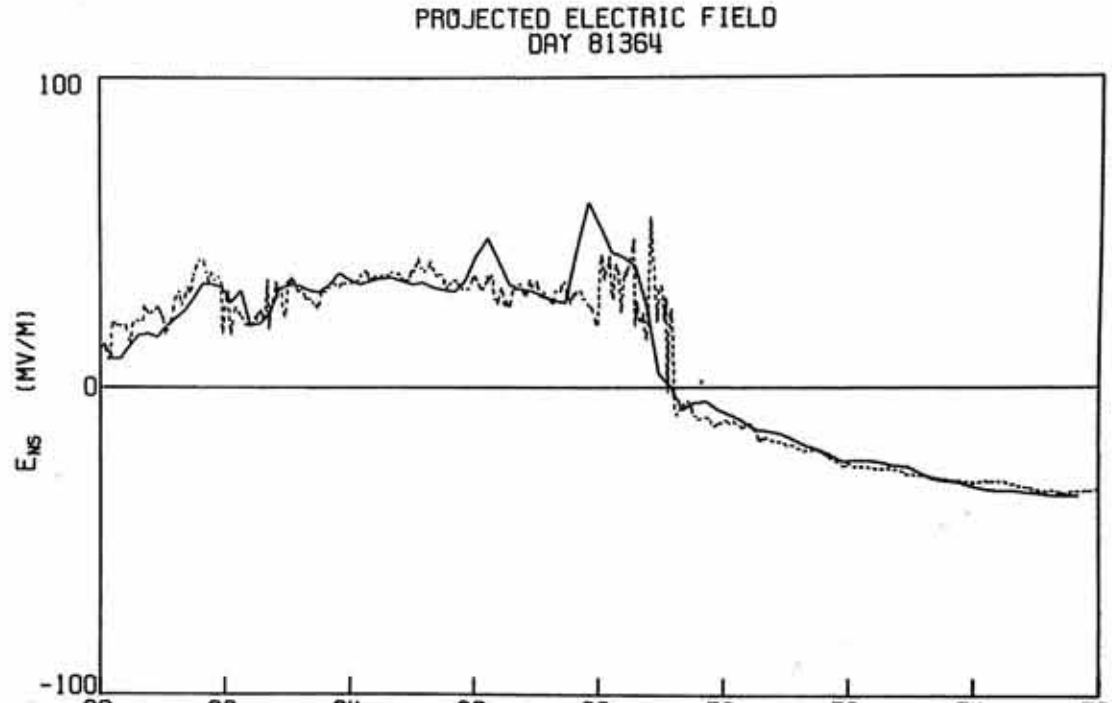

INV LAT	60	62	64	66	68	70	72	74	76
UT.DE-1	09:16	09:15	09:14	09:14	09:13	09:12	09:12	09:11	09:10
UT.DE-2	09:19	09:19	09:18	09:17	09:17	09:16	09:16	09:15	09:14
ΔT	+00:03	+00:03	+00:03	+00:03	+00:03	+00:04	+00:04	+00:04	+00:04
ALT.DE-1(KM)	2122	1949	1798	1661	1537	1424	1320	1227	1141
ALT.DE-2(KM)	659	671	682	693	704	715	726	737	747
MLT.DE-1(HR)	4.62	4.64	4.65	4.67	4.69	4.72	4.75	4.80	4.86
MLT.DE-2(HR)	4.66	4.67	4.69	4.72	4.75	4.78	4.83	4.89	4.98

Figure 2

Figure 3 Projected electric fields measured by DE-1 and DE-2 on day 296 (October 23), 1981. Positive electric fields are in the southernly direction.

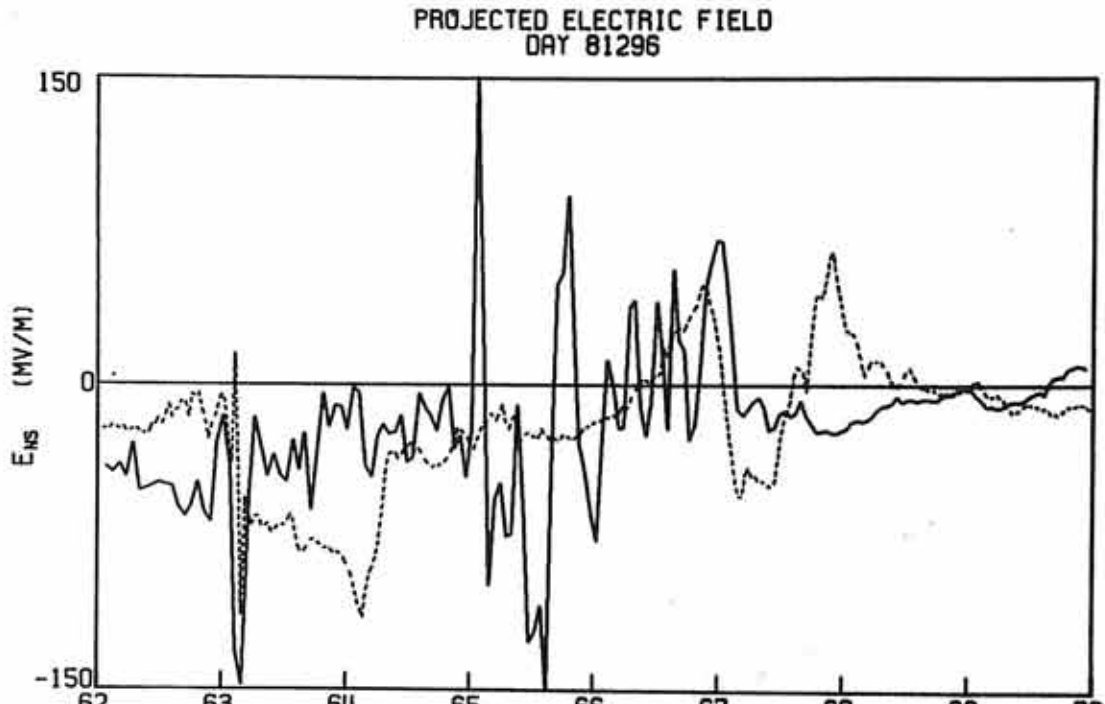

INV LAT	62	63	64	65	66	67	68	69	70
UT.DE-1	03:49	03:48	03:46	03:45	03:43	03:42	03:40	03:39	03:37
UT.DE-2	04:02	04:01	04:01	04:01	04:00	04:00	04:00	04:00	03:59
ΔT	+00:12	+00:13	+00:14	+00:15	+00:17	+00:18	+00:19	+00:20	+00:22
ALT.DE-1(KM)	8173	8436	8707	8987	9277	9576	9885	10205	10536
ALT.DE-2(KM)	896	899	903	906	909	912	915	917	921
MLT.DE-1(HR)	20.41	20.39	20.36	20.34	20.31	20.29	20.26	20.23	20.20
MLT.DE-2(HR)	20.00	19.96	19.92	19.87	19.83	19.78	19.72	19.66	19.59

Figure 3

Figure 4 Electric field spectrums from day 296 (October 23), 1981. The spectrums are obtained from a Fourier transform of the electric field data between 62° and 67° invariant latitude. The solid line shows the spectrum of the electric field measured by DE-1. The solid line shows the spectrum of the electric field measured by DE-2. The ordinate values are obtained from the square root of the "spectral power density." The actual units are mV m^{-1} $\sqrt{k_m}$.

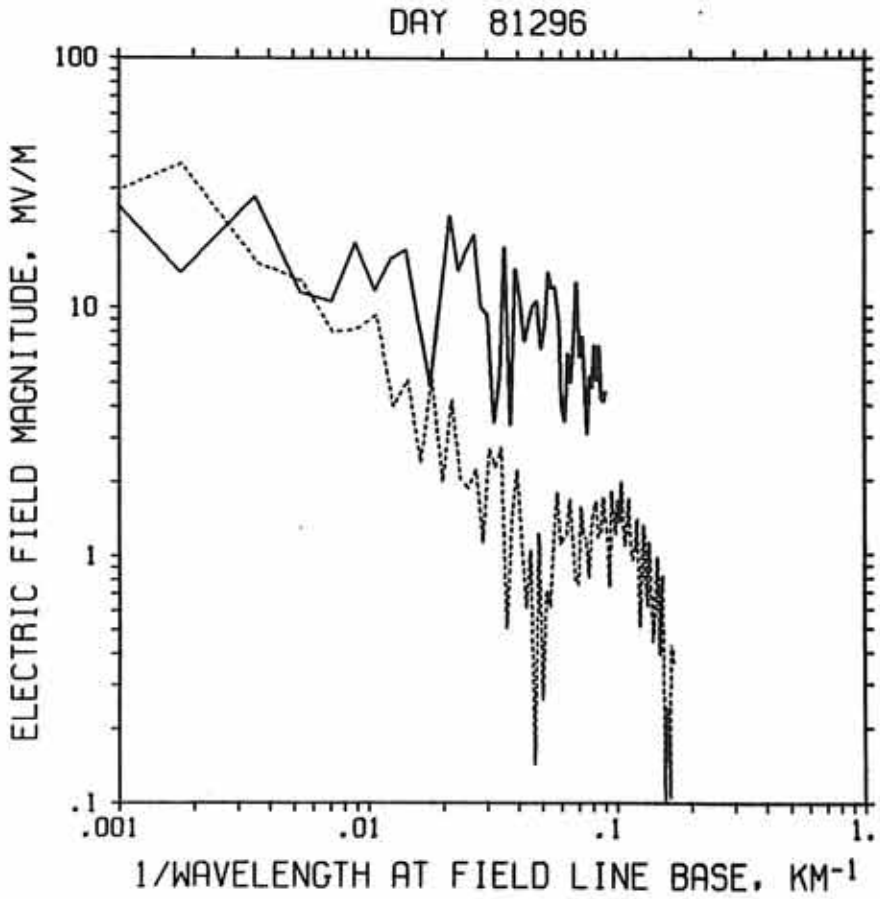

INVARIANT LATITUDE
62 - 67

TIME

DE-1	3:42:28 - 3:49:16
DE-2	4: 0:39 - 4: 2:13

ALTITUDE

DE-1	9570 - 8201 KM
DE-2	912 - 896 KM

MLT

DE-1	20.29 - 20.41 HR
DE-2	19.78 - 20.00 HR

Figure 4

Figure 5 Results of electron measurements from the High Altitude Plasma Instrument on day 296 (October 23), 1981. The top panel shows the Pedersen conductivity which is calculated from the measured electron flux.

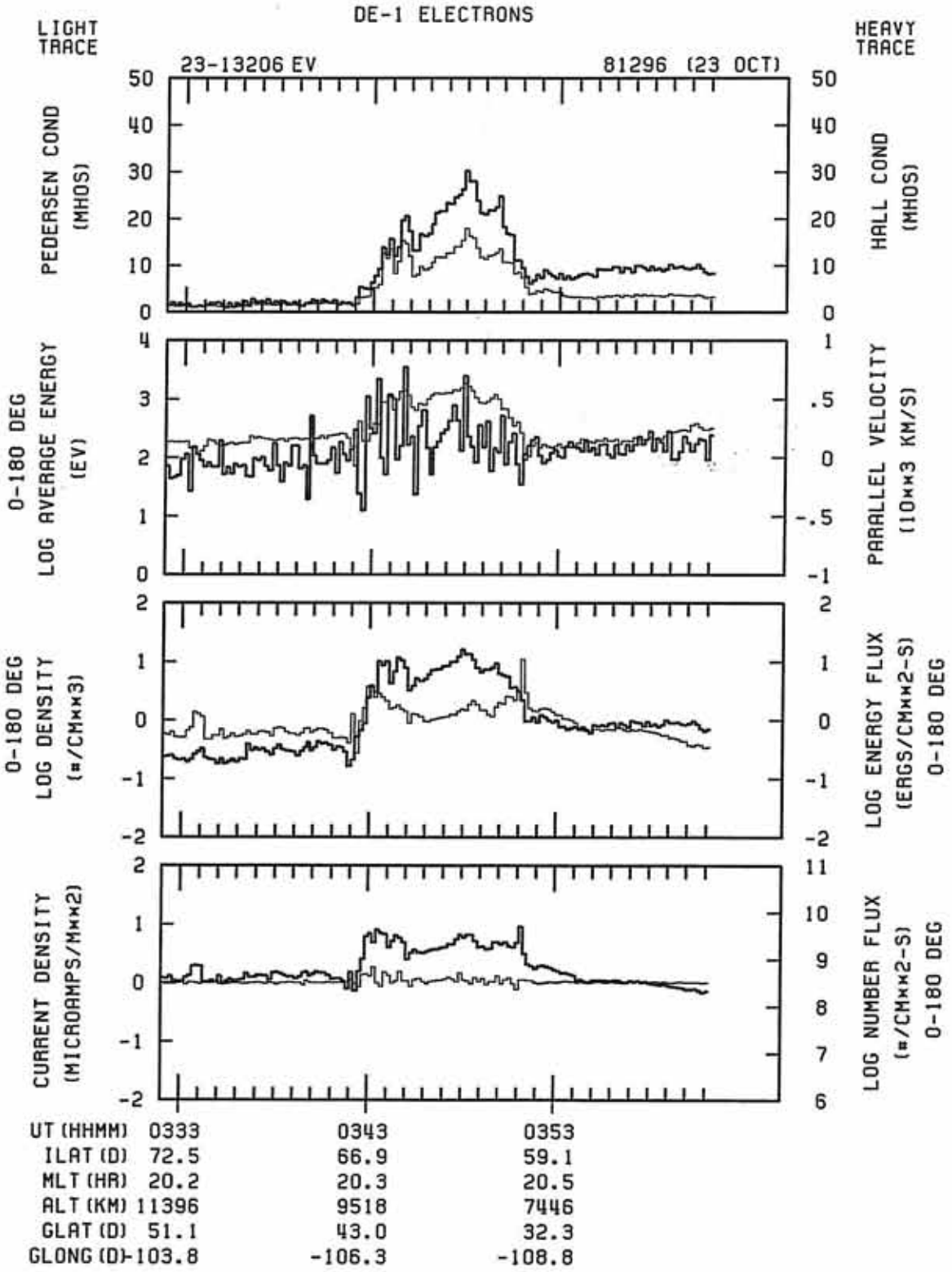
DE-1 ELECTRONS
LIGHT TRACE
HEAVY TRACE
23-13206 EV
81296 (23 OCT)
PEDERSEN COND (MHOS)
HALL COND (MHOS)
0-180 DEG LOG AVERAGE ENERGY (EV)
PARALLEL VELOCITY (10**3 KM/S)
0-180 DEG LOG DENSITY (#/CM**3)
LOG ENERGY FLUX (ERGS/CM**2-S) 0-180 DEG
CURRENT DENSITY (MICROAMPS/M**2)
LOG NUMBER FLUX (#/CM**2-S) 0-180 DEG
UT (HHMM) 0333 0343 0353
ILAT (D) 72.5 66.9 59.1
MLT (HR) 20.2 20.3 20.5
ALT (KM) 11396 9518 7446
GLAT (D) 51.1 43.0 32.3
GLONG (D) -103.8 -106.3 -108.8

Figure 5

Figure 6 East-west magnetic field measured by the magnetometer on DE-1 on day 296 (October 23), 1981, from 3:40 UT to 3:55 UT. The middle panel shows the current density which is obtained from the derivative of the magnetic field. For comparison, the north-south electric field is shown on the bottom panel. All data are shown without multiplication by a projection factor.

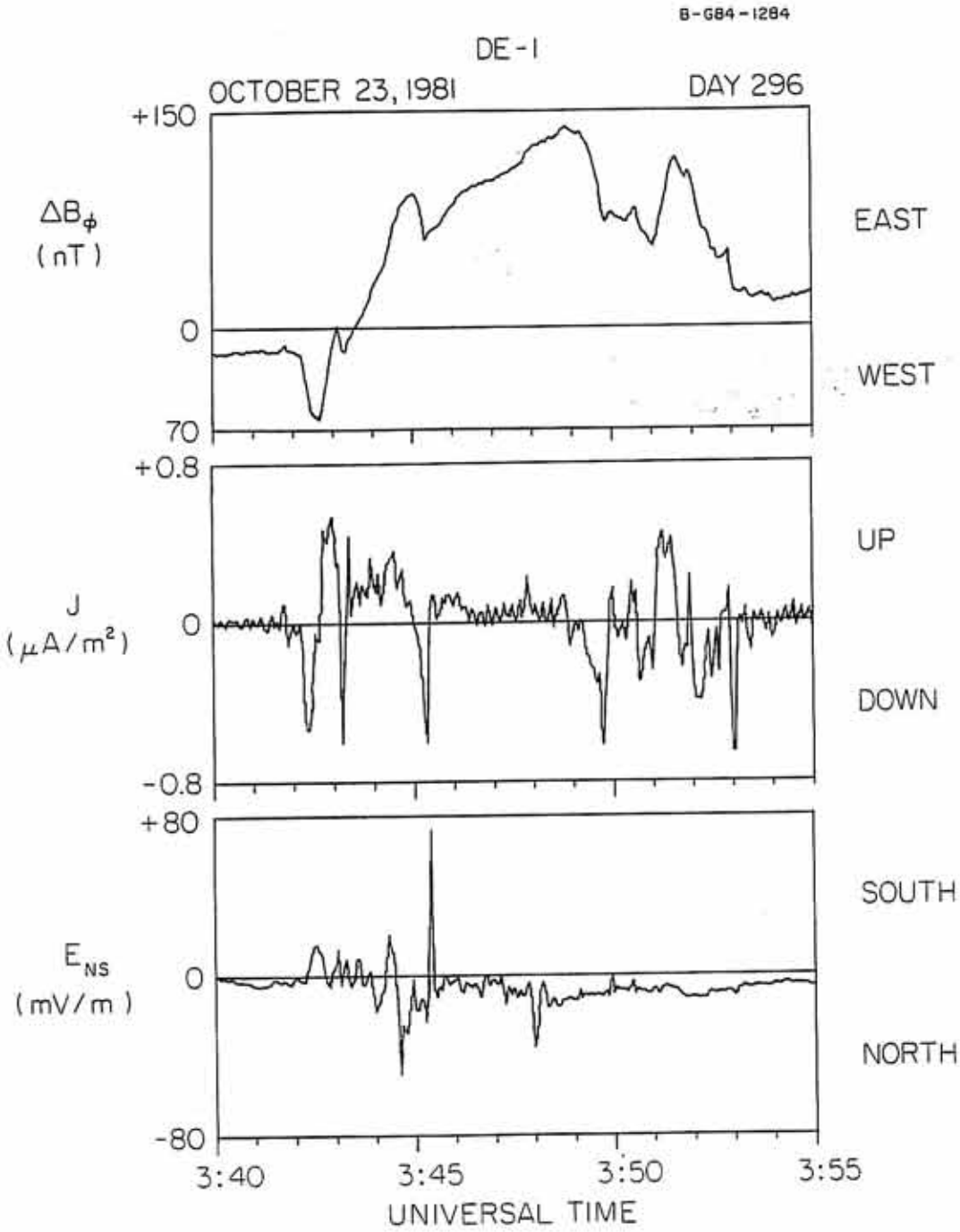
B-G84-1284
DE-I
OCTOBER 23, 1981
DAY 296
+150
ΔB_ϕ
(nT)
0
70
EAST
WEST
+0.8
J
(μA/m^2)
0
-0.8
UP
DOWN
+80
E_{NS}
(mV/m)
0
-80
SOUTH
NORTH
3:40
3:45
3:50
3:55
UNIVERSAL TIME

Figure 6

Figure 7 Magnetic field spectrum from day 296 (October 23), 1981. The solid line shows the Fourier transform of the east-west magnetic field data (DE-1) between 62° and 67° invariant latitude. For comparison, it is shown superimposed on the electric field spectrum measured by DE-2 (dashed line) at a lower altitude. The ratio is approximately constant at all wavelengths.

A-G84-1308

OCTOBER 23, 1981 DAY 296
62° TO 67° INVARIANT LATITUDE

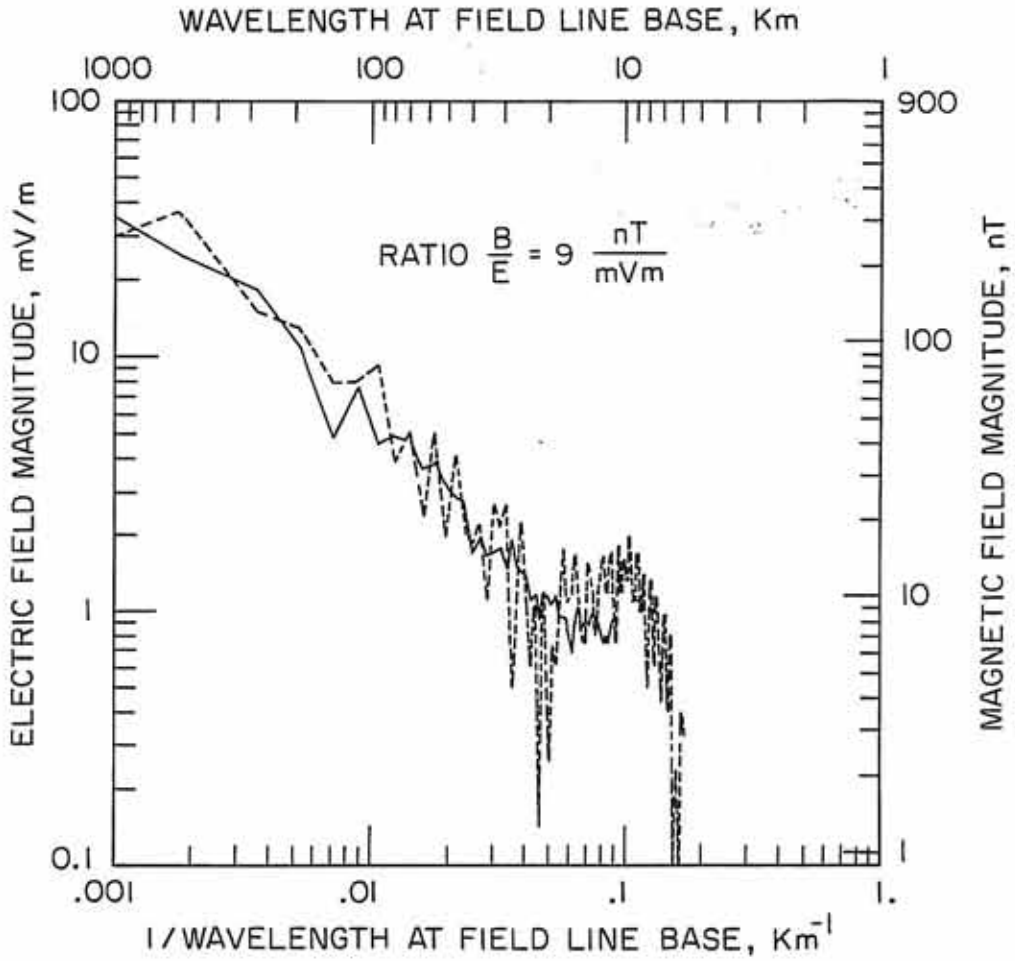

Figure 7

Figure 8 Projected electric fields measured by DE-1 and DE-2 on day 303 (October 30), 1981. The solid line shows the DE-1 electric field and the dashed line shows the DE-2 electric field.

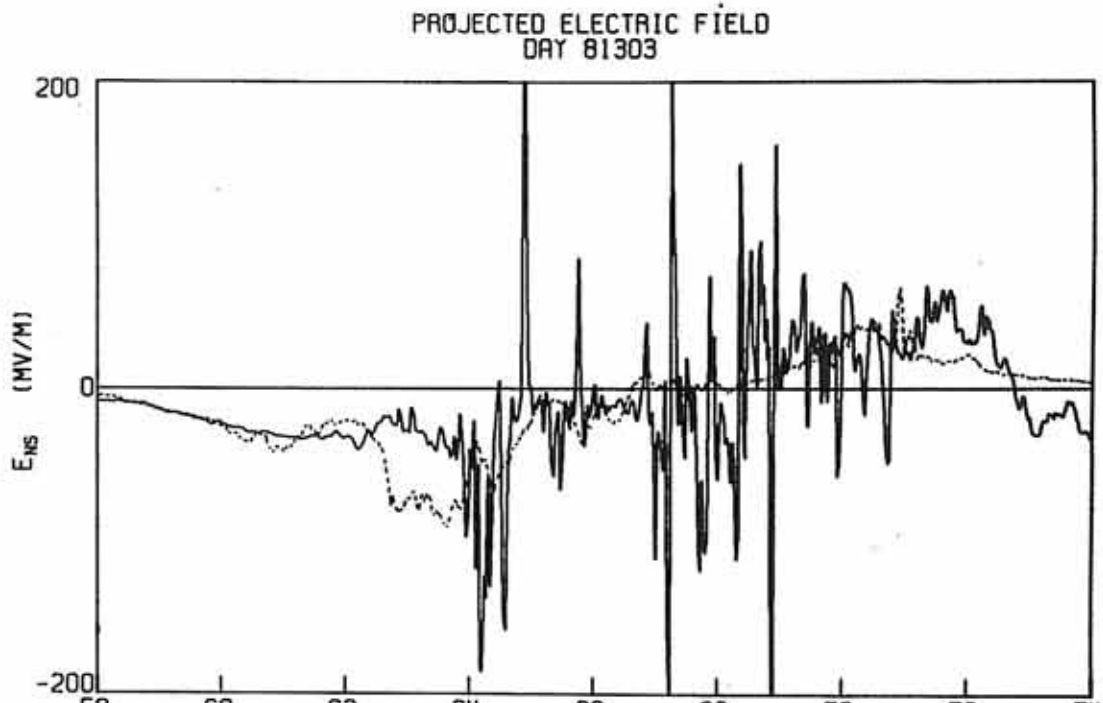

INV LAT	58	60	62	64	66	68	70	72	74
UT.DE-1	13:46	13:43	13:39	13:35	13:31	13:26	13:20	13:14	13:07
UT.DE-2	13:58	13:57	13:57	13:56	13:55	13:55	13:54	13:53	13:53
ΔT	+00:11	+00:14	+00:17	+00:20	+00:24	+00:28	+00:33	+00:39	+00:45
ALT.DE-1(KM)	9205	9849	10537	11269	12050	12881	13764	14699	15677
ALT.DE-2(KM)	831	840	849	859	867	875	883	891	898
MLT.DE-1(HR)	20.64	20.65	20.65	20.66	20.66	20.66	20.66	20.65	20.64
MLT.DE-2(HR)	20.79	20.82	20.84	20.87	20.90	20.94	20.98	21.03	21.09

Figure 8

Figure 9 Electric field spectrums from day 303 (October 30), 1981, 65° to 70° invariant latitude.

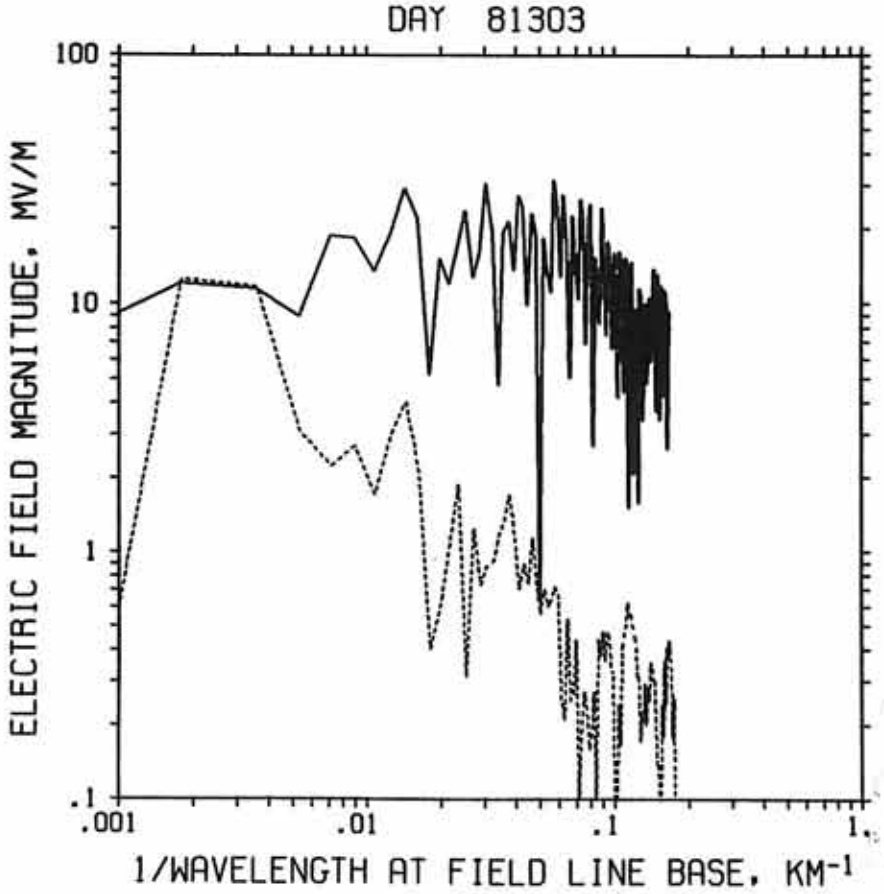

INVARIANT LATITUDE
65 - 70

TIME
DE-1 13:20:57 - 13:33:29
DE-2 13:54:36 - 13:56:15

ALTITUDE
DE-1 13743 - 11654 KM
DE-2 883 - 863 KM

MLT
DE-1 20.66 - 20.66 HR
DE-2 20.98 - 20.88 HR

Figure 9

Figure 10 Results of electron measurements from the High Altitude Plasma Instrument on day 303 (October 30), 1981.

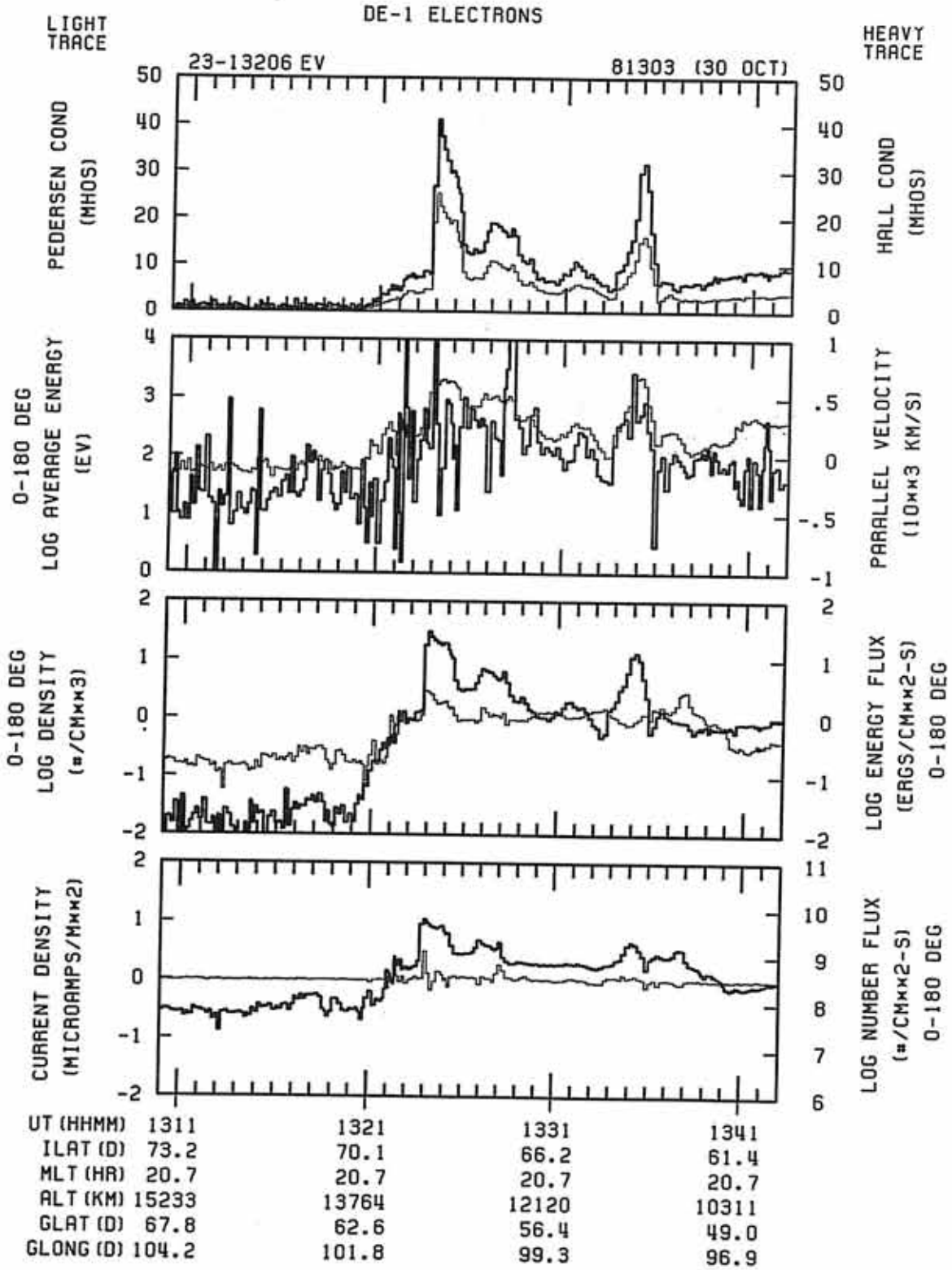
DE-1 ELECTRONS
LIGHT TRACE
HEAVY TRACE
23-13206 EV
81303 (30 OCT)
PEDERSEN COND (MHOS)
HALL COND (MHOS)
0-180 DEG LOG AVERAGE ENERGY (EV)
PARALLEL VELOCITY (10**3 KM/S)
0-180 DEG LOG DENSITY (#/CM**3)
LOG ENERGY FLUX (ERGS/CM**2-S) 0-180 DEG
CURRENT DENSITY (MICROAMPS/M**2)
LOG NUMBER FLUX (#/CM**2-S) 0-180 DEG
UT (HHMM) 1311 1321 1331 1341
ILAT (D) 73.2 70.1 66.2 61.4
MLT (HR) 20.7 20.7 20.7 20.7
ALT (KM) 15233 13764 12120 10311
GLAT (D) 67.8 62.6 56.4 49.0
GLONG (D) 104.2 101.8 99.3 96.9

Figure 10

Figure 11 East-west magnetic field measured by the magnetometer on DE-1 on day 303 (October 30), 1981, from 13:19 UT to 13:40 UT. The middle panel shows the current density and the bottom panel shows the electric field without projection.

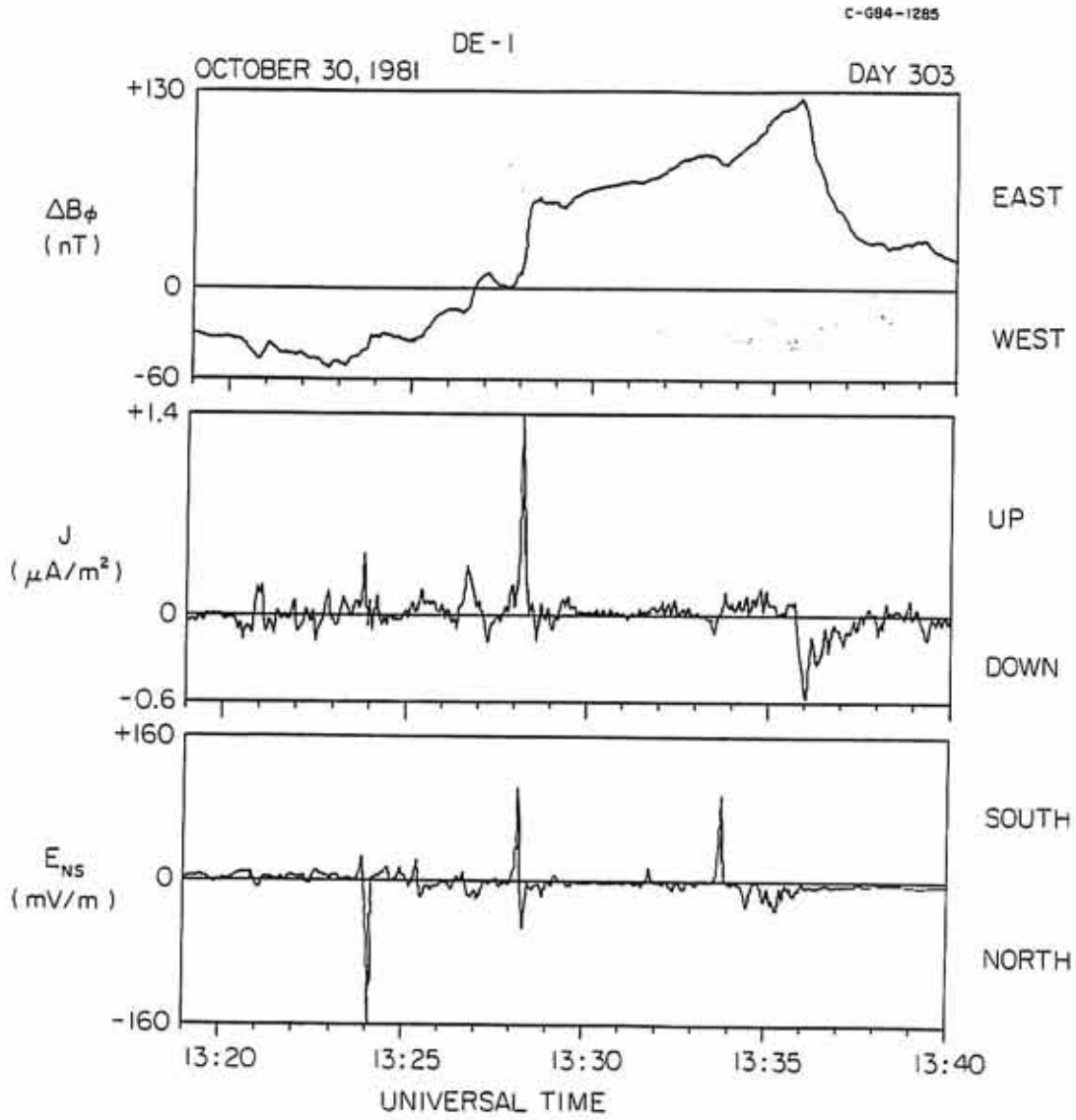
C-G84-1285
DE-1
OCTOBER 30, 1981
DAY 303
+130
ΔBφ
(nT)
0
-60
EAST
WEST
+1.4
J
(μA/m²)
0
-0.6
UP
DOWN
+160
E_NS
(mV/m)
0
-160
SOUTH
NORTH
13:20
13:25
13:30
13:35
13:40
UNIVERSAL TIME

Figure 11

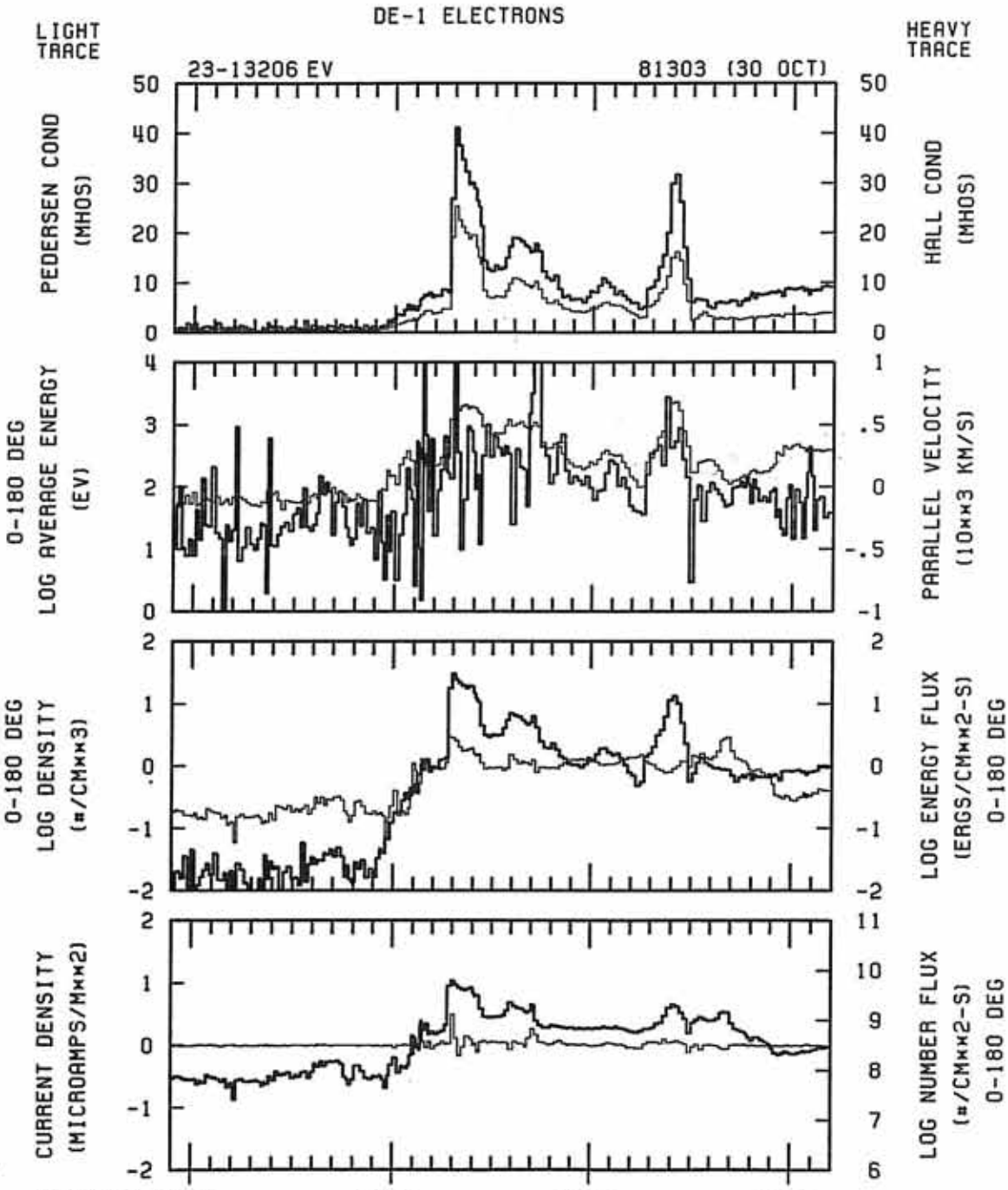

UT (HHMM)	1311	1321	1331	1341
ILAT (D)	73.2	70.1	66.2	61.4
MLT (HR)	20.7	20.7	20.7	20.7
ALT (KM)	15233	13764	12120	10311
GLAT (D)	67.8	62.6	56.4	49.0
GLONG (D)	104.2	101.8	99.3	96.9

Figure 10

Figure 11 East-west magnetic field measured by the magnetometer on DE-1 on day 303 (October 30), 1981, from 13:19 UT to 13:40 UT. The middle panel shows the current density and the bottom panel shows the electric field without projection.

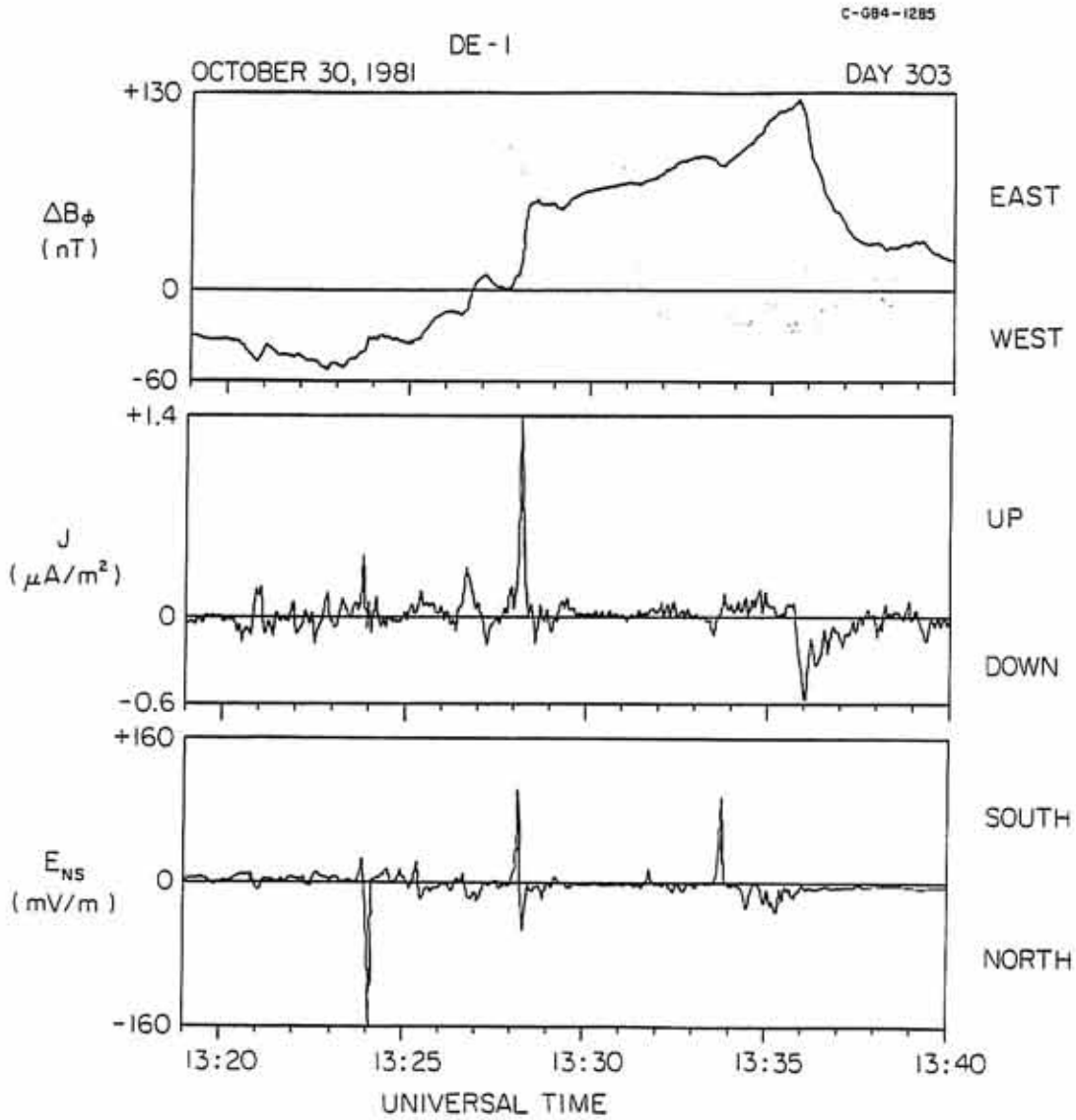
C-G84-1285
DE-1
OCTOBER 30, 1981
DAY 303
+130
ΔBφ
(nT)
0
-60
EAST
WEST
+1.4
J
(μA/m²)
0
-0.6
UP
DOWN
+160
E_NS
(mV/m)
0
-160
SOUTH
NORTH
13:20
13:25
13:30
13:35
13:40
UNIVERSAL TIME

Figure 11

Figure 12 Magnetic field spectrum from day 303 (October 30), 1981. The data are from 65° to 70° invariant latitude. The solid line is the DE-1 magnetic field spectrum and the dashed line is the DE-2 electric field spectrum. As in the previous case, the ratio is nearly constant.

A-G84-1309

OCTOBER 30, 1981 DAY 303
65° TO 70° INVARIANT LATITUDE

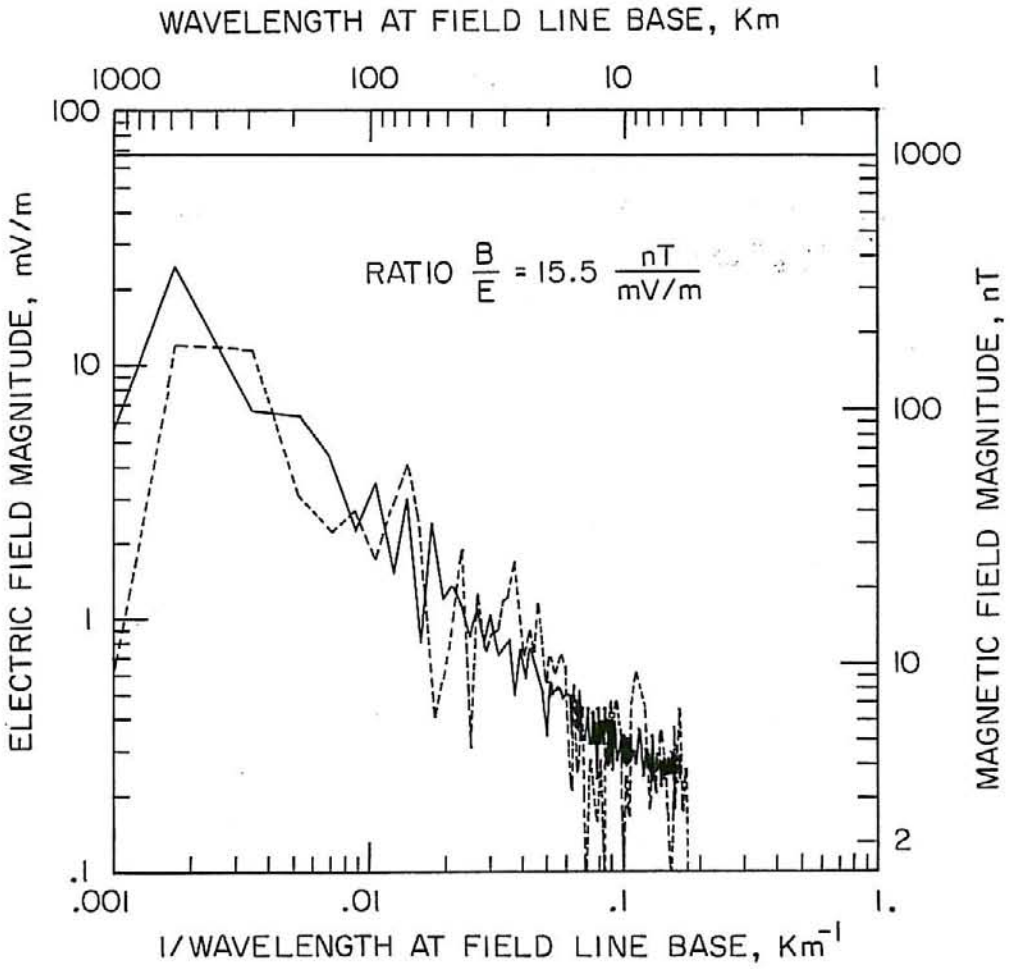

Figure 12

Figure 13 Electric field spectrum forms from day 303 (October 30), 1981, 55° to 60° invariant latitude.

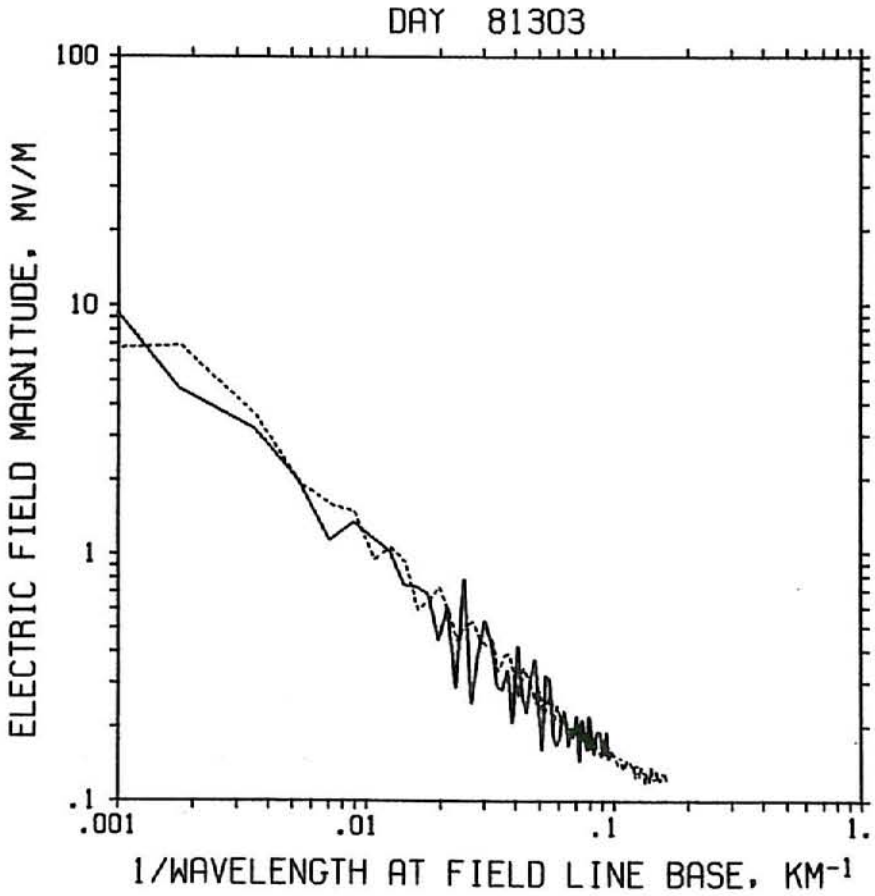

INVARIANT LATITUDE
55 - 60

TIME

DE-1	13:43:29 - 13:50:49
DE-2	13:57:51 - 13:59:23

ALTITUDE

DE-1	9800 - 8334 KM
DE-2	840 - 816 KM

MLT

DE-1	20.65 - 20.63 HR
DE-2	20.82 - 20.76 HR

Figure 13

Figure 14 Average electric fields measured by DE-1 and DE-2 as a function of invariant latitude. The data are from 18 different cases where there was a magnetic conjunction within the range of 40° to 80° invariant latitude, and DE-I was at radial distances greater than 1.7 R_e. The data had been Fourier transformed for each 5° of invariant latitude and then divided into four different frequency ranges before averaging. The values are actually from the square-root of the spectral power density. Note that while the two spacecraft measure nearly identical electric fields at the largest wavelengths, the high altitude satellite (DE-1) measures much larger electric fields at the shorter wavelengths, especially between 60° and 75°. All electric fields had been projected to 1 R_e.

C-G84-1263

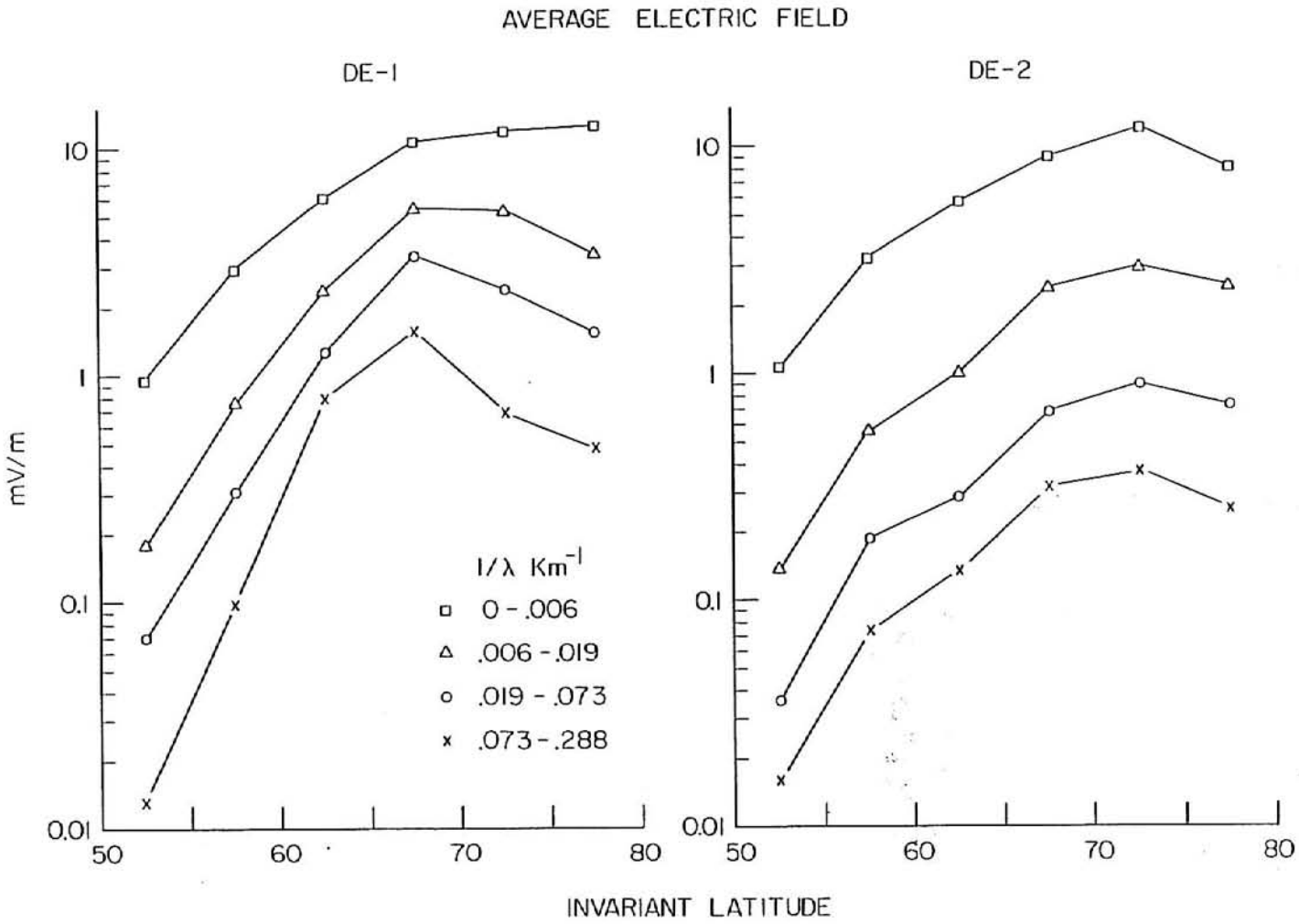

Figure 14

Figure 15 Average electric fields measured by DE-1 and DE-2 as a function of wavelength. The data set is the same as in Figure 14, although only from 65° to 70° invariant latitude. Averages were taken in eight different frequency (wavelength) bins. The ratio of the low altitude electric field (E_2) divided by the high altitude electric field (E_1) drops as the wavelength gets smaller.

A-G84-1279

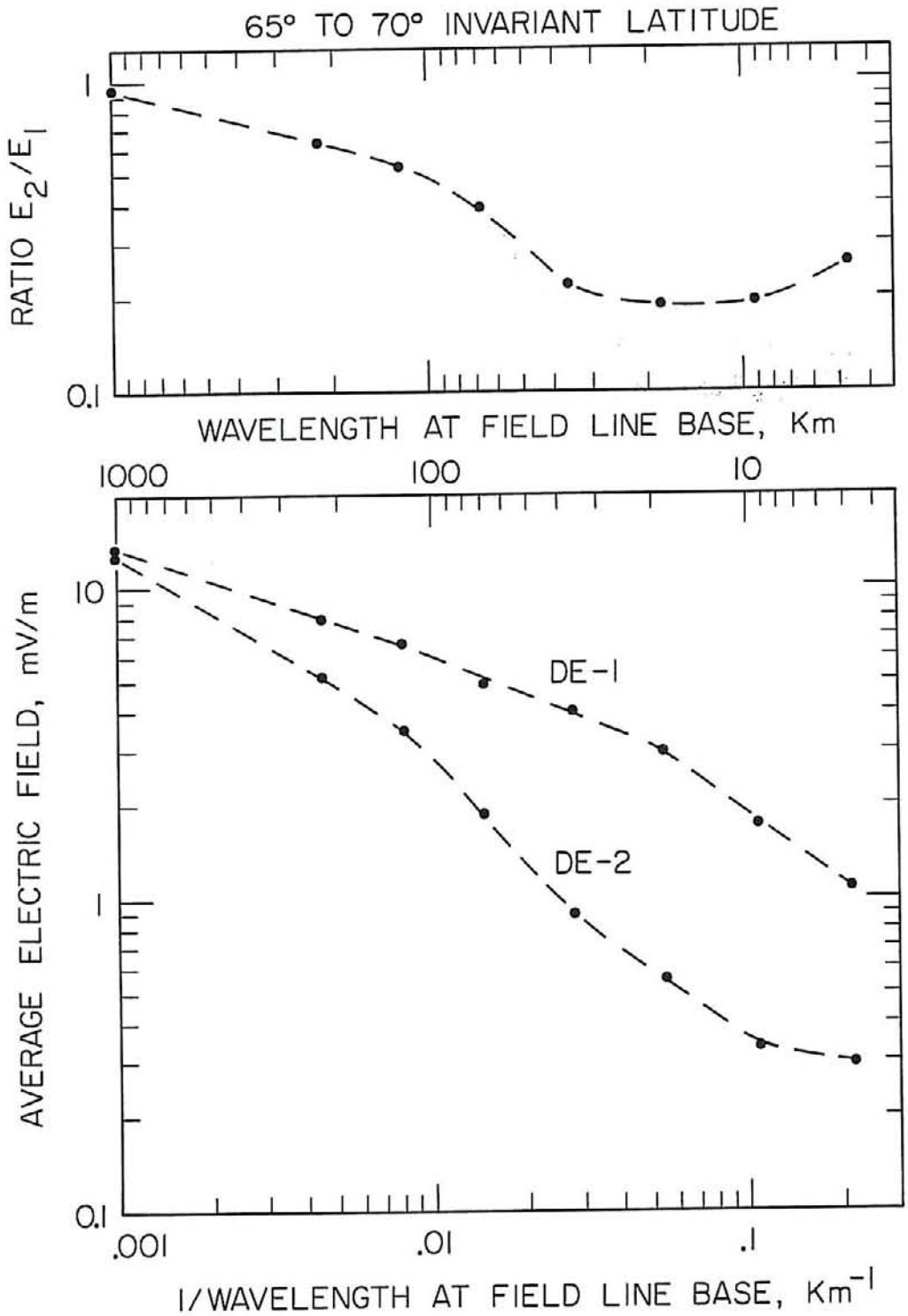

Figure 15

Figure 16 Definition of coordinates used in mathematical derivations.

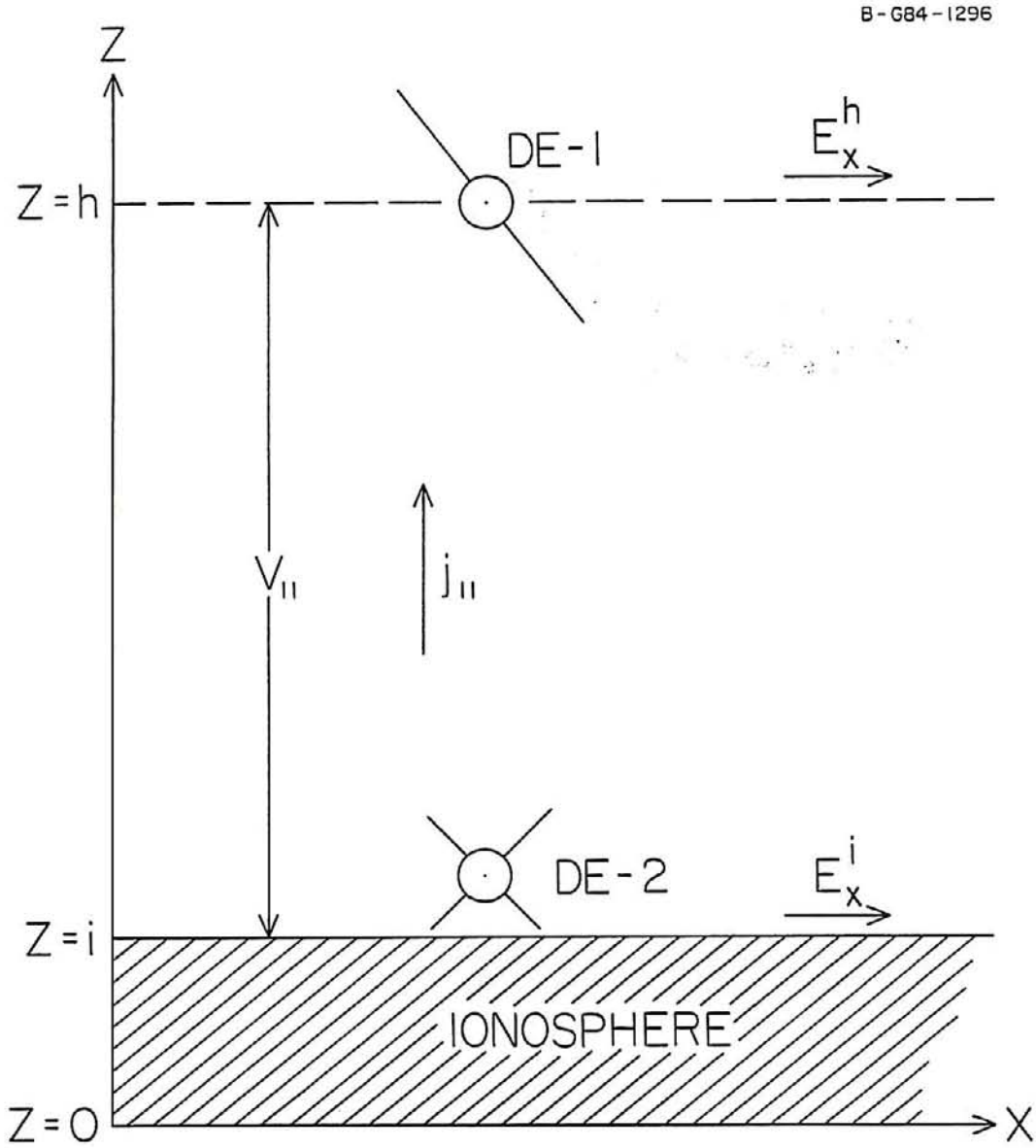
B-G84-1296
Z
DE-1
E_x^h
Z=h
$V_{\parallel}$
$j_{\parallel}$
DE-2
E_x^i
Z=i
IONOSPHERE
Z=0
X

Figure 16

Figure 17 Plot of E_2/E_1 ratio vs. wavelength, from the electric field spectrums on day 296, 1981. The dashed line shows the best visual fit of the theoretical curve to the data points. The value of k_o is determined by the best fit.

A-G84-1297

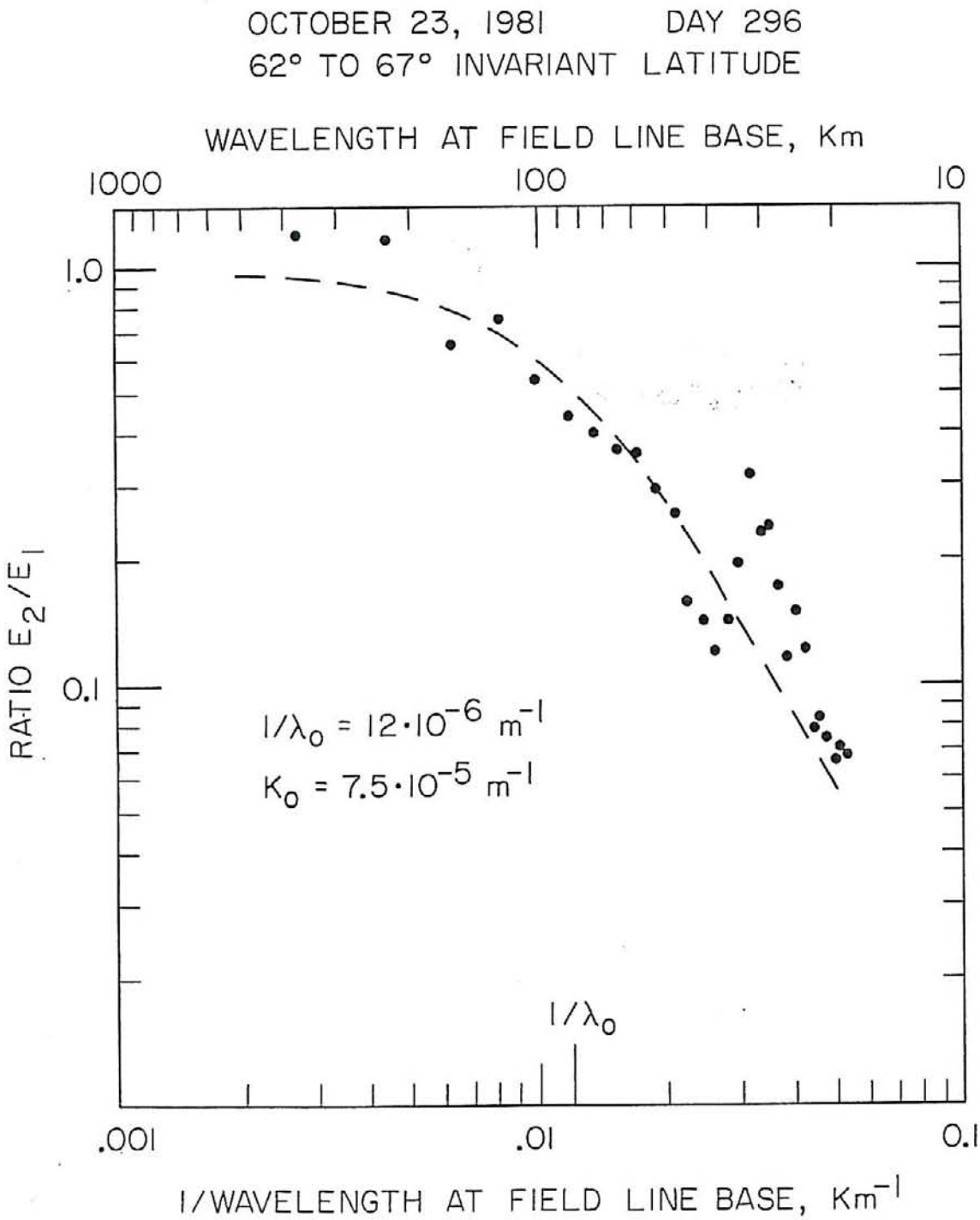

Figure 17

Figure 18 Plot of E_2/E_1 ratio vs. wavelength, from the electric field spectrums on day 303, 1981.

A-G84-1298

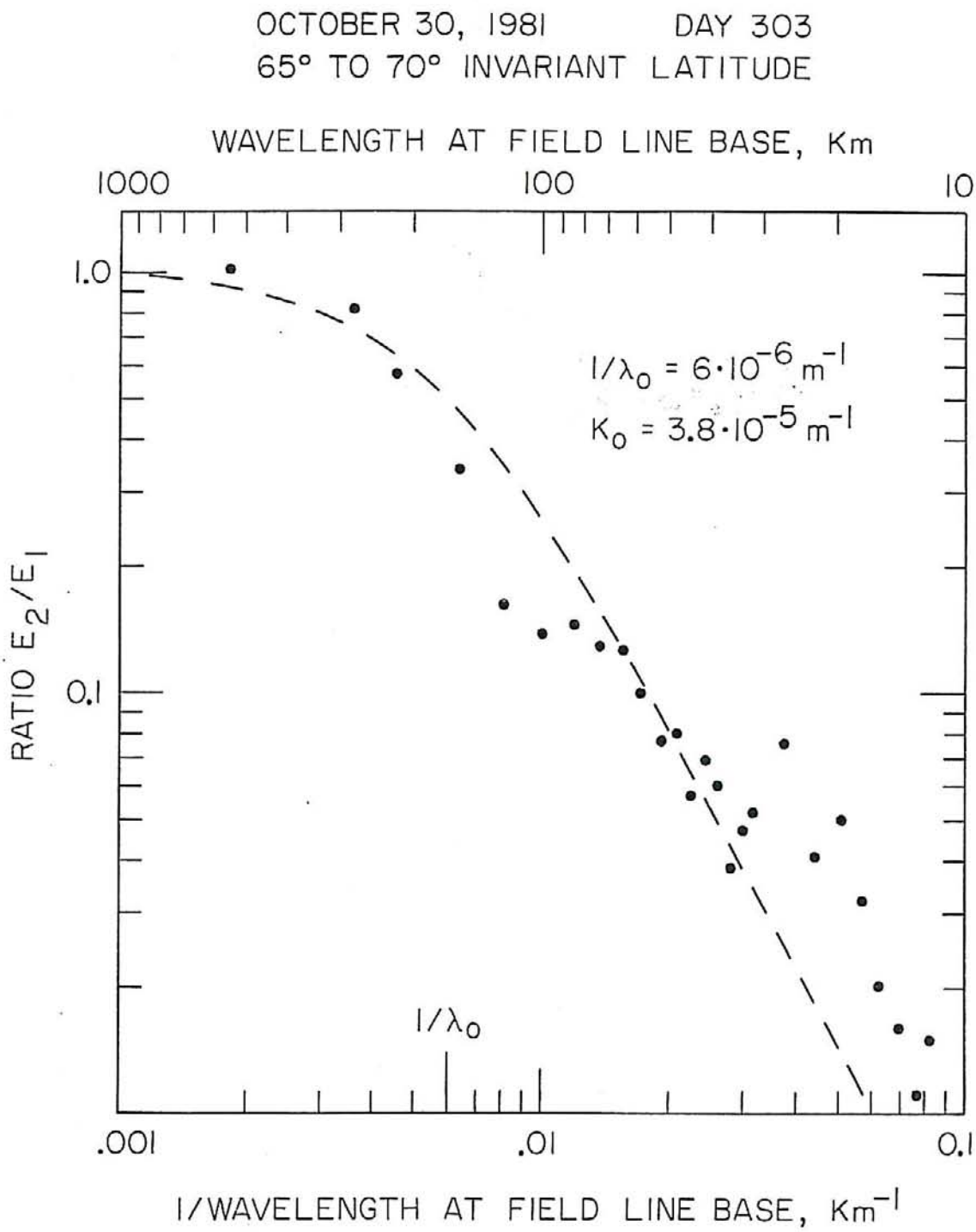

Figure 18

Figure 19 Plot of ratio $j_{\parallel}/E_x^h$ vs. wavelength, from the DE-1 electric and magnetic field spectrums on day 296, 1981. The dashed line is not the result of a best fit, but was computed from the values of Σ_p and k_o which were determined by other means.

A-G84-1304

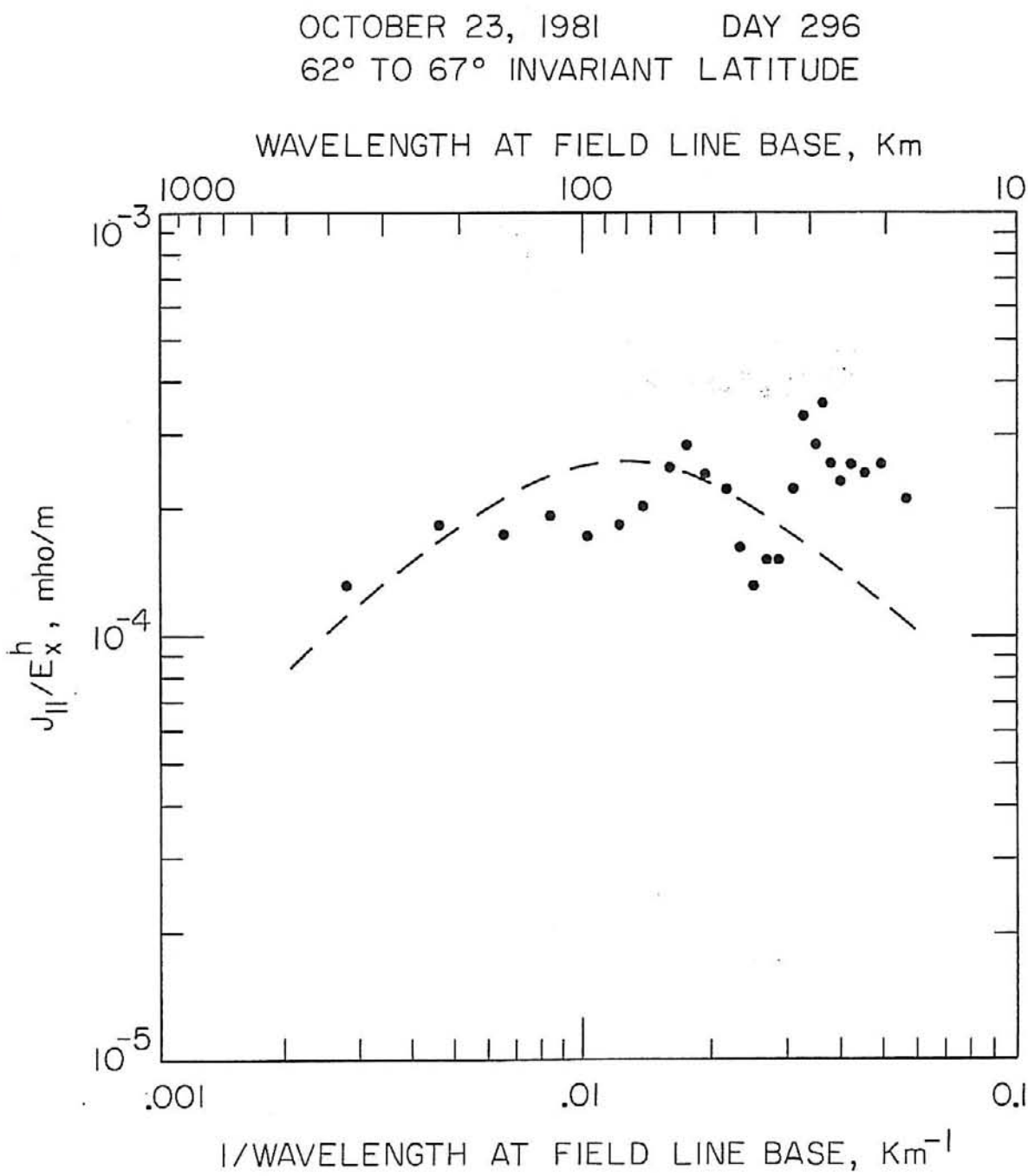

Figure 19

Figure 20 Plot of ratio $j_{\parallel}/E_x^h$ vs. wavelength, from the DE-1 electric and magnetic field spectrums on day 303, 1981. As in Figure 19, the dashed line was computed from parameters which were determined by other techniques.

A-G84-1305

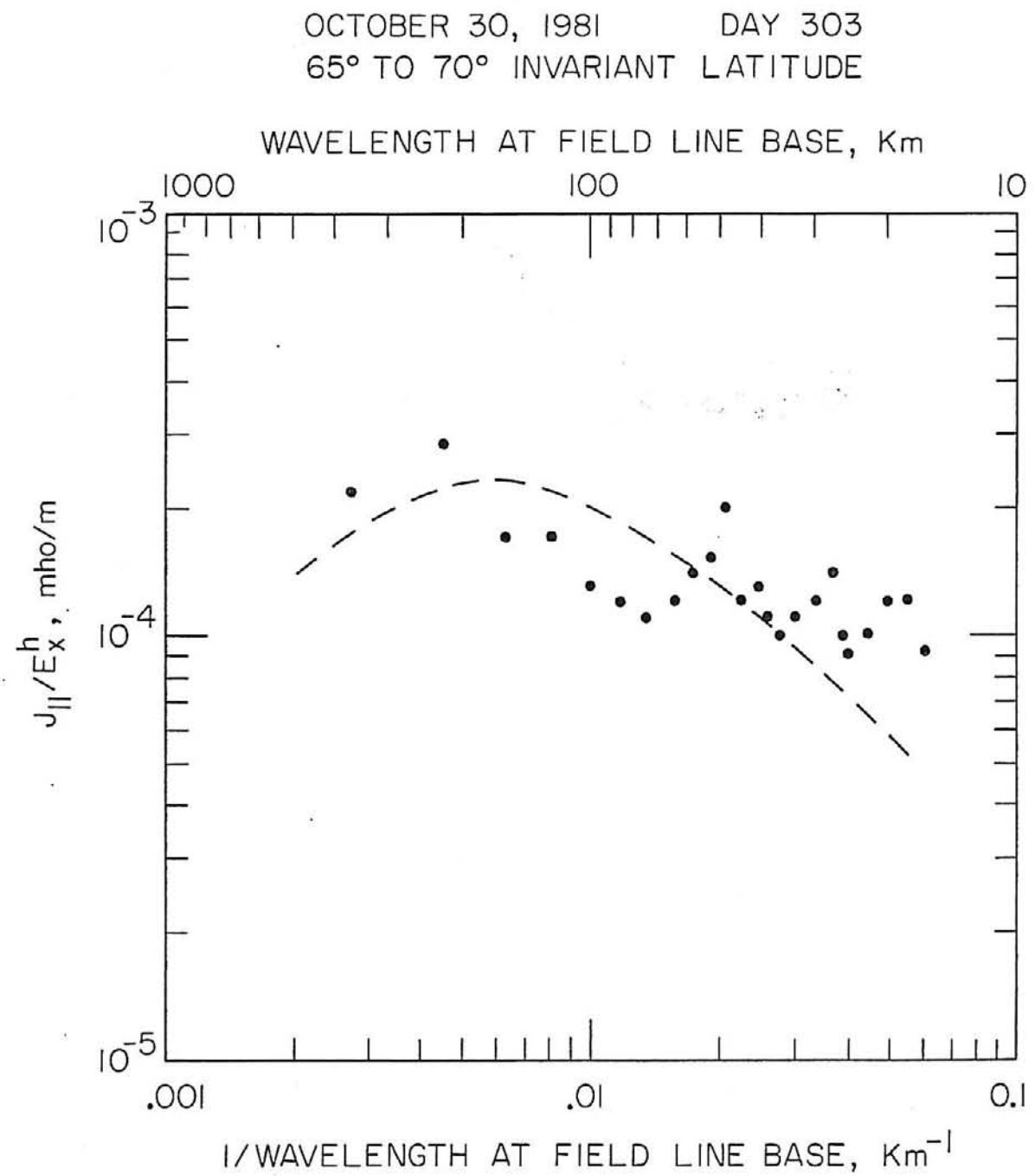

Figure 20

REFERENCES

Aggson, T. L., J. P. Heppner, and N. C. Maynard, Observations of large magnetospheric electric fields during the onset phase of a substorm, J. Geophys. Res., 88, 3981, 1983.

Arnoldy, R. L., R. L. Kaufmann, L. J. Cahill, and S. B. Mende, PC 1 pearl-electron interactions on the L = 4.2 magnetic shell, Geophys. Res. Lett., 10, 8, 627, 1983.

Batchelor, B. K., The Theory of Homogeneous Turbulence, Cambridge University Press, New York, 1970.

Burch, J. L., J. D. Winningham, V. A. Blevins, N. Eaker, W. C. Gibson, and R. A. Hoffman, High-Altitude Plasma Instrument for Dynamics Explorer-A, Space Sci. Instr., 5, 455, 1981.

Burke, W. J., M. S. Gussenhoven, M. C. Kelley, D. A. Hardy, and F. J. Rich, Electric and magnetic field characteristics of discrete arcs in the polar cap, J. Geophys. Res., 87, 2431, 1982.

Cauffman, D. P., and D. A. Gurnett, Satellite measurements of high latitude convection electric fields, Space Science Reviews, 13, 369, 1972.

Chiu, Y. T., and J. M. Cornwall, Electrostatic model of a quiet auroral arc, J. Geophys. Res., 85, 543, 1980.

Chiu, Y. T., A. L. Newman, and J. M. Cornwall, On the structure and mapping of auroral electrostatic potentials, J. Geophys. Res., 86, 10,029, 1981.

Dubinin, E. M., P. L. Israelevich, N. S. Nikoleava, I. Kutiev, and I. M. Podgorny, Localized auroral disturbance in the morning sector of topside ionosphere as a standing electromagnetic wave, English preprint from Academy of Sciences of the USSR Space Research Institute, submitted to Planet. Space Sci., 1984.

Fahleson, U., Theory of electric field measurements conducted in the magnetosphere with electric probes, Space Science Reviews, 7, 238, 1967.

Farthing, W. H., M. Sugiura, B. G. Ledley, and L. J. Cahill, Magnetic field observations on DE-A and -B, Space Sci. Instr., 5, 551, 1981.

Gelpi, C. G., and E. A. Bering, The plasma wave environment of an auroral arc: 2. ULF waves on an auroral arc boundary, J. Geophys. Res., paper 4A1112, 1984.

Goertz, C. K., and R. W. Boswell, Magnetosphere-ionosphere coupling, J. Geophys. Res., 84, 7239, 1979.

Gurnett, D. A., and L. A. Frank, A region of intense plasma wave turbulence on auroral field lines, J. Geophys. Res., 82, 1031, 1977.

Gurnett, D. A., R. L. Huff, J. D. Menietti, J. D. Winningham, J. L. Burch, and S. D. Shawhan, Correlated low frequency electric and magnetic noise along the auroral field lines, J. Geophys. Res., 89, 8971, 1984.

Hasegawa, A., Particle acceleration by MHD surface wave and formation of aurora, J. Geophys. Res., 81, 5083, 1976.

Hoffman, R. A., and E. R. Schmerling, Dynamics Explorer program: An overview, Space Sci. Instr., 5, 345, 1981a.

Hoffman, R. A., G. D. Hogan, and R. C. Maehl, Dynamics Explorer spacecraft and ground operations systems, Space Sci. Instr., 5, 349, 1981b.

Kintner, P. M., Observations of velocity shear driven plasma turbulence, J. Geophys. Res., 81, 5114, 1976.

Knight, S., Parallel electric fields, Planet. Space Sci., 21, 741, 1973.

Langel, R. A., R. H. Estes, G. D. Mead, E. B. Fabiano, and E. R. Lancaster, Initial geomagnetic field model from Magsat vector data, Geophys. Res. Lett., 7, 10, 793, 1980.

Lyons, L. R., Generation of large-scale regions of auroral currents electric potentials, and precipitation by divergence at the convection electric fields, J. Geophys. Res., 85, 17, 1980.

Lyons, L. R., Discrete aurora as the direct result of an inferred high-altitude generating potential distribution, J. Geophys. Res., 86, 1, 1981.

Lysak, R. L., and C. W. Carlson, The effect of microscopic turbulence on magnetosphere-ionosphere coupling, Geophys. Res. Lett., 8, 269, 1981.

Lysak, R. L., and C. T. Dum, Dynamics of magnetosphere-ionosphere coupling including turbulent transport, J. Geophys. Res., 88, 365, 1983.

Lysak, R. L., and M. K. Hudson, Coherent anomalous resistivity in the region of electrostatic shocks, Geophys. Res. Lett., 6, 8, 661, 1979.

Mallinckrodt, A. J., and C. W. Carlson, Relations between transverse electric fields and field-aligned currents, J. Geophys. Res., 83, 1426, 1978.

Maynard, N. C., E. A. Bielecki, and H. F. Burdick, Instrumentation for vector electric field measurements from DE-B, Space Sci. Instr., 5, 523, 1981.

Maynard, N. C., J. P. Heppner, and T. L. Aggson, Turbulent electric fields in the nightside magnetosphere, J. Geophys. Res., 87, 1445, 1982.

Maynard, N. C., J. P. Heppner, and A. Egeland, Intense variable electric fields at ionospheric altitudes in the high latitude regions as observed by DE-2, Geophys. Res. Lett., 9, 9, 981, 1982.

Mozer, F. S., C. W. Carlson, M. K. Hudson, R. B. Tobert, B. Parady, and J. Yatteau, Observations of paired electrostatic shocks in the polar magnetosphere, Phys. Rev. Lett., 38, 6, 292, 1977.

Mozer, F. S., C. A. Cattell, M. K. Hudson, R. L. Lysak, M. Temerin, and R. B. Torbert, Satellite measurements and theories of low altitude auroral particle acceleration, Space Sci. Rev., 27, 155, 1980.

Mozer, F. S., and R. B. Tobert, An average parallel electric field deduced from the latitude and altitude variations of the perpendicular electric field below 8000 kilometers, Geophys. Res. Lett., 7, 3, 219, 1980.

Shawhan, S. D., D. A. Gurnett, D. A. Odem, R. A. Helliwell, and C. G. Park, The Plasma Wave Instrument and Quasi-Static Electric Field Instrument (PWI) for Dynamics Explorer-A, Space Sci. Instr., 5, 535, 1981.

Shawhan, S. D., C.-G. Fälthammar, and L. P. Block, On the nature of large auroral zone electric fields at 1-R_e altitude, J. Geophys. Res., 83, 1049, 1978.

Shelley, E. G., D. A. Simpson, T. C. Sanders, E. Hertzberg, H. Balsiger, and A. Ghielmetti, The Energetic Ion Composition Spectrometer (EICS) for the Dynamics Explorer-A, Space Sci. Instr., 5, 443, 1981.

Smiddy, M., W. J. Burke, M. C. Kelley, N. A. Saflekos, M. S. Gussenhoven, D. A. Hurdy, and F. J. Rich, Effects of high-latitude conductivity on observed convection electric fields and Birkeland currents, J. Geophys. Res., 85, 6811, 1980.

Stern, D. P., One-dimensional models of quasi-neutral parallel electric fields, J. Geophys. Res., 86, 5839, 1981.

Stern, D. P., Electric currents and voltage drops along auroral field lines, Space Sci. Rev., 34, 317, 1983.

Sugiura, M., A fundamental magnetosphere-ionosphere coupling mode involving field-aligned currents as deduced from DE-2 observations, Geophys. Res. Lett., 11, 9, 877, 1984.

Sugiura, M., N. C. Maynard, W. H. Farthing, J. P. Heppner, and B. G. Ledley, Initial results on the correlation between the magnetic and electric fields observed from the DE-2 satellite in the field-aligned current regions, Geophys. Res. Lett., 9, 9, 985, 1982.

Weimer, D. R., Magnetospheric electric fields measured with Dynamics Explorer-1, University of Iowa Dept. of Physics and Astronomy, M.S. Thesis, 1983.